HELIUM IN THE TERRESTRIAL ATMOSPHERE

G. KOCKARTS

Institut d'Aéronomie Spatiale de Belgique, 1180 Bruxelles, Belgium

(Received 18 April, 1973)

Abstract. After a brief historical review of the discovery of helium in the terrestrial atmosphere, the production mechanisms of the isotopes He^4 and He^3 are discussed. Although the radioactive production of He^4 in the Earth is well understood, some uncertainty still exists for the degassing process leading to an atmospheric influx of $(2.5 \pm 1.5) \times 10^6$ atoms cm^{-2} s^{-1}. Different production mechanisms are possible for He^3 leading to an influx of (7.5 ± 2.5) atoms cm^{-2} s^{-1}. Observations of helium in the thermosphere show a great variability of this constituent. The different mechanisms proposed to explain the presence of the winter helium bulge are discussed. Since helium ions are present in the topside ionosphere and in the magnetosphere, ionization mechanisms are analyzed. Owing to possible variations and uncertainties in the solar UV flux, the photoionization coefficient is $(8 \pm 4) \times 10^{-8}$ s^{-1}. Finally, the helium balance between production in the earth and loss into the interplanetary space is discussed with respect to the different processes which can play an effective role.

1. Introduction

Unlike the other inert gases of the periodic system, helium was not discovered through its presence in the Earth's atmosphere. One century ago several astronomers (Janssen, 1868; Frankland and Lockyer, 1869; Secchi, 1868) found an unexplained emission line in the solar spectrum near the sodium doublet lines. This new line was attributed to a new constituent of the Sun by Rayet (1869) and a few years later the name *helium* ($\eta\lambda\iota o\varsigma$ = Sun) appeared in the scientific literature.

The presence of helium on the Earth was first established by Ramsay (1895) from a spectroscopic analysis of the gases extracted from a uranium mineral. In the same year, Kayser (1895) analyzed the natural outgassing of spring water and detected helium, thereby indicating its presence as a natural atmospheric constituent.

Around 1900, considerable effort was devoted to the determination of the chemical composition of air. Owing to the relatively low abundances of the rare gases, it was rather difficult to obtain accurate absolute values. The first reliable estimate of the atmospheric helium abundance was made by Ramsay (1905, 1908) and led to a volume mixing ratio of 4×10^{-6}. Later, Watson (1910) obtained the value 5.4×10^{-6} which is almost identical with the presently accepted value of 5.24×10^{-6} (Glückauf, 1946).

Since helium is present at ground level, Chapman and Milne (1920) investigated its possible effect on the composition of the atmosphere at great heights. Figure 1 shows the result obtained by Chapman and Milne (1920) when diffusive equilibrium was assumed above 20 km altitude. Although we know today that this figure is quantitatively incorrect, it illustrates the idea that diffusion can increase the helium mixing ratio from its small ground level value up to a value of unity with an altitude variation of a few hundreds of kilometers. Chapman and Milne (1920) discussed also the effect of a height change of the diffusion level. Several years later, Jeans (1925)

Space Science Reviews **14** (1973) 723–757.

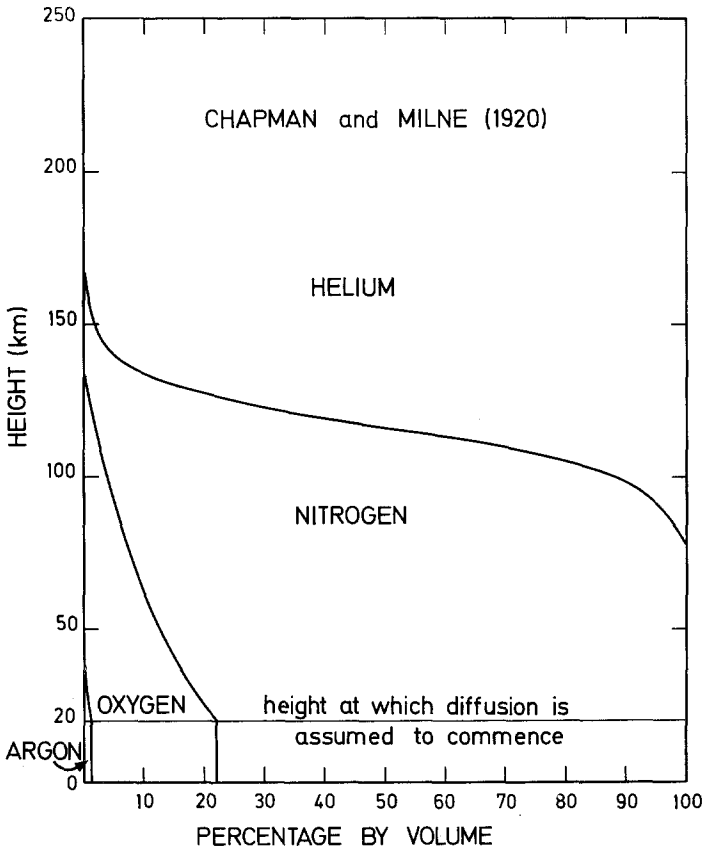

Fig. 1. Abundance of molecular nitrogen, molecular oxygen, argon and helium. This figure is redrawn from Chapman and Milne (1920).

concluded that with an abundance of 10^{-4} for H_2 at ground level, hydrogen should also be present in the upper atmosphere, becoming the major atmospheric constituent above 75 km. The difficulty of deciding whether hydrogen or helium, or both, were important constituents of the upper atmosphere came from a lack of observational evidence, particularly with regard to the possibility of auroral emissions. Furthermore, the hydrodynamical character of the upper atmosphere was not well enough known to permit even an approximate determination of the level where diffusive equilibrium began.

The first attempt (Glückauf and Paneth, 1946) to determine the height at which helium gravitational separation begins was made with air samples collected from 20 to 25 km altitude. The results showed that at least up to 25 km height, the relative composition of the atmosphere was unaffected by gravitational separation of its constituents. With the scientific use of rockets after the Second World War, it became clear that molecular diffusion begins to be effective around 100 km altitude. Mass spectrometric measurements (Meadows and Towsend, 1958; Pokhunkov, 1962) of

the concentration ratio $n(Ar)/n(N_2)$ showed that a transition from perfect mixing towards diffusive separation occurs in the altitude region between 100 km and 120 km. Analysis of the atmospheric turbulence near 100 km by means of artificial sodium clouds releases (Blamont and De Jager, 1961; Blamont and Baguette, 1961) led to the same conclusion. Even now, however, a detailed knowledge of processes within this transition region is sparse and considerable uncertainty must exist in any theoretical model of the transition from the mixing conditions of the homosphere to the diffusive conditions present in the heterosphere.

Experimental and theoretical interest in the problem of atmospheric helium was renewed when Nicolet (1961) indicated that helium is an important constituent in the lower exosphere. Today, more than fifty years after the pioneering work of Chapman and Milne (1920), helium and its associated physical phenomena are still subject to intense research. The number of observational facts has considerably increased and the theoretical approach has become increasingly sophisticated. Nevertheless answers to many problems surrounding the presence of helium in the upper atmosphere have not yet been found. In the following sections discussions are given of the various factors which affect helium in the Earth's atmosphere.

2. Helium-4 Production Rate

It is now well established that the atmospheric helium-4 is a consequence of degassing from the Earth's crust and of the mantle where He^4 is produced by radioactive decay of thorium and of uranium according to the following processes:

$$Th^{232} \rightarrow Pb^{208} + 6\ He^4 \tag{1}$$

$$U^{235} \rightarrow Pb^{207} + 7\ He^4 \tag{2}$$

$$U^{238} \rightarrow Pb^{206} + 8\ He^4. \tag{3}$$

The appropriate decay constants are respectively $\lambda_{232} = 4.98 \times 10^{-11}\ yr^{-1}$, $\lambda_{235} = 9.74 \times 10^{-10}\ yr^{-1}$, and $\lambda_{238} = 1.54 \times 10^{-10}\ yr^{-1}$. With the present crustal isotopic abundances of Th = 100%, $U^{238}:U^{235}:U^{234} = 99.27:0.72:0.006\%$, the number of He^4 atoms produced in one second per g of Th and of U is respectively $P_{Th} = 2.46 \times 10^4$ atoms $g^{-1}\ s^{-1}$ and $P_U = 1.02 \times 10^5$ atoms $g^{-1}\ s^{-1}$. When M(Th) and M(U) are respectively the total masses of thorium and of uranium contained in the Earth, the total production of He^4 atoms per second is

$$P(He^4) = P_{Th}\, M(Th) + P_U\, M(U). \tag{4}$$

The determination of the effective rate at which helium enters the atmosphere requires, however, the solution of two fundamental problems; i.e., the exact amount of uranium and of thorium present within the earth must be known and the fraction of the produced helium which actually enters into the atmosphere must also be determined. The basic aspects of the degassing problem will now be discussed in relation with the amount of Ar^{40} present in the Earth's atmosphere.

2.1. Degassing coefficient

Turekian (1959) introduced a method for computing a degassing coefficient from the existing amount of argon-40 in the terrestrial atmosphere. It is known that argon-40 results from radioactive decay of potassium-40 which can also produce calcium-40. Assuming that all terrestrial Ar^{40} results from the decay of primordial K_0^{40} the total content of argon-40 in the Earth is then given by

$$\frac{d\,Ar_E^{40}}{dt} = \lambda_{40} K_0^{40} e^{-\lambda_{40} t} - \delta\, Ar_E^{40}, \tag{5}$$

where δ is the degassing coefficient, t is the time measured from the Earth's origin, $\lambda_{40} = 5.21 \times 10^{-10}$ yr^{-1} is the decay constant of K^{40}, and K_0^{40} is the primordial abundance of potassium-40 which leads to the production of argon-40. K_0^{40} is related to the primordial total abundance of potassium-40 $K_0^{40}(\text{tot})$ by

$$K_0^{40} = R K_0^{40}(\text{tot})/(1 + R), \tag{6}$$

where $R = 0.11$ (e.g. Heydemann, 1969) is the branching ratio between the production of Ar^{40} and Ca^{40}. When $Ar_E^{40} = 0$ for $t = 0$, integration of (5) leads to

$$Ar_E^{40}(t)/K_0^{40} = \frac{\lambda_{40}}{\delta - \lambda_{40}} (e^{-\lambda_{40} t} - e^{-\delta t}) \tag{7}$$

and the amount of atmospheric argon Ar_A^{40} resulting from degassing is then given by

$$\frac{d\,Ar_A^{40}}{dt} = \delta Ar_E^{40}. \tag{8}$$

Since argon is unable to escape from the Earth's gravitational field, the existing amount of argon in the atmosphere is obtained by integration of (8) from $t = 0$ till $t_E = 4.55 \times 10^9$ yr,

$$Ar_A^{40}(t_E) = \frac{K_0^{40}}{\delta - \lambda_{40}} [\delta (1 - e^{-\lambda_{40} t_E}) - \lambda_{40} (1 - e^{-\delta t_E})]. \tag{9}$$

For conditions of standard temperature and pressure, an atmospheric argon mixing ratio of 9.34×10^{-3} leads to an atmospheric total content of 1.93×10^{23} atoms cm^{-2}. The total amount of argon-40 present in the atmosphere is then 9.84×10^{41} atoms or 6.53×10^{19} g. Knowing K_0^{40} in Equation (9) it is possible to determine the degassing coefficient δ by an iterative procedure. K_0^{40} can be computed from the present total abundance of potassium [K], since the present isotopic abundance K^{40} is 1.19×10^{-4}. Figure 2 gives the degassing coefficient as a function of the present abundance [K] in g/g. The dashed curve corresponds to the case where the potassium abundance refers to the entire earth (crust + mantle + core). The full curve corresponds to the case where argon production occurs only in the crust and in the mantle. When the abundance of the entire Earth is multiplied by 1.47 (Earth mass/crust + mantle mass),

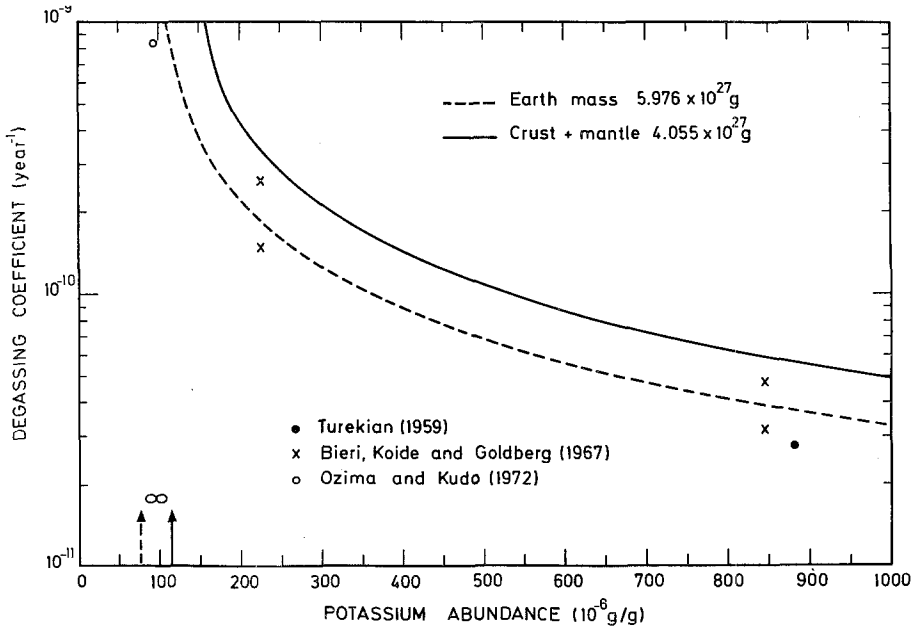

Fig. 2. Degassing coefficient δ as a function of the present total abundance of potassium.

one obtains the abundance for the crust and for the mantle leading to the same degassing coefficient. Values obtained by Turekian (1959) and by Bieri *et al.* (1967) for a chondritic potassium abundance are also indicated on Figure 2.

In an analysis of the thermal balance of the Earth, Wasserburg *et al.* (1964) suggest that terrestrial materials are characterized by a ratio $[K]/[U] \sim 10^4$ which is eight times smaller than the ratio $[K]/[U] \sim 8 \times 10^4$ usually observed in chondrite meteorites. Under these conditions the degassing coefficient increases approximately by a factor of 5. Bieri *et al.* (1967) used such a non-chondritic model in their computations of the helium outflow. Any diminution of the potassium abundance corresponds to an increase of the degassing coefficient, since a smaller amount of potassium has to supply the same amount of existing atmospheric argon.

While Bieri *et al.* (1967) used the method proposed by Turekian (1959) to evaluate the degassing coefficient, Ozima and Kudo (1972) recently deduced a degassing coefficient of 8.5×10^{-10} yr^{-1} from an analysis of the time variation of the isotopic ratio Ar^{40}/Ar^{36}. In addition a potassium abundance of 9.6×10^{-5} g g^{-1} is uniquely determined from this analysis; i.e. a value which is approximately a factor of 10 smaller than the potassium abundance in chondrites. The degassing coefficient of Ozima and Kudo (1972) is, however, not incompatible with the results shown on Figure 2. To see this, we note that from Equation (9)

$$\delta \to \infty \text{, when } A_r^{40}(t_E)/K_0^{40} = 1 - e^{-\lambda_{40} t_E}. \tag{10}$$

For the entire Earth, the condition given by (10) leads to a present abundance $[K] =$

$= 7.85 \times 10^{-5}$ g g^{-1} while for the crust and the mantle alone, one obtains $[K] = 1.16 \times 10^{-4}$ g g^{-1}. These values, indicated by arrows on Figure 2, can be considered as lower limits of the present potassium abundance based on a theory with time independent degassing coefficient. The lower limits deduced from equation (10) are also consistent with the low potassium abundance $[K] = (1.3 \pm 0.4) \times 10^{-4}$ g g^{-1} inferred by Larimer (1971) from comparison between crustal and meteoritic abundances.

2.2. Helium-4 outflow

Essentially three methods have been used to evaluate the helium-4 outflow from the Earth's surface.

(1) By measuring the ratio He^4/Ar^{40} in numerous natural gases and by estimating the Ar^{40} flux, Wasserburg *et al.* (1963) deduced a helium-4 outflow of 3.2×10^6 atoms $cm^{-2}\ s^{-1}$.

(2) By computing the He^4 production through processes (1) to (3) and by noting that the amounts of terrestrial thorium and uranium must be compatible with the thermal balance of the Earth, Nicolet (1957) deduced a He^4 flux of 1.74×10^6 atoms $cm^{-2}\ s^{-1}$. In addition, the abundances $[U] = 1.19 \times 10^{-8}$ g g^{-1} and $[Th] = 3.95 \times 10^{-8}$ g g^{-1} have been determined by Morgan and Lovering (1967) for carbonaceous chondrites. With a mass of 4.055×10^{27} g for the crust and the mantle, relation (4) leads to a production of 8.86×10^{24} atoms s^{-1}. For an Earth surface area of 5.1×10^{18} cm^2, such a production corresponds to 1.74×10^6 atoms $cm^{-2}\ s^{-1}$ which is identical with the flux obtained by Nicolet (1957).

(3) The third method, introduced by Turekian (1959), is based on equations similar to (5) and (8) for helium, after the degassing coefficient has been obtained as shown previously.

Before discussing results obtained by this method, however, it is necessary to examine briefly how the helium production is related to the thermal balance of the earth. With the isotopic abundances and the heat productions of Table I (see Heydemann, 1969), the amount of heat (erg $g^{-1}\ s^{-1}$) presently produced within the Earth is given by

$$Q = 3.32 \times 10^{-5}[K] + 2.65 \times 10^{-1}[Th] + 9.76 \times 10^{-1}[U], \qquad (11)$$

where [K], [Th] and [U] are respectively the present abundances in g/g of potassium, thorium and uranium. A material with chondritic composition ($[K] = 8.45 \times 10^{-4}$ g g^{-1}, $[Th] = 3.95 \times 10^{-8}$ g g^{-1} and $[U] = 1.19 \times 10^{-8}$ g g^{-1}) leads then to a heat

TABLE I

Radioactive heat production

	K^{40}	Th^{232}	U^{235}	U^{238}
Isotopic abundance (present time)	1.19×10^{-4}	1	7.2×10^{-3}	9.927×10^{-1}
Heat release (erg $g^{-1}\ s^{-1}$)	0.279	0.265	5.71	0.942

production of 5.014×10^{-8} erg g^{-1} s^{-1}. For a mantle and a crust characterized by such a chondritic composition, the heat flow is 40 erg cm^{-2} s^{-1}. The mean global heat flow measured at ground level is 63 erg cm^{-2} s^{-1} (see Schmucker, 1969) whereas the normal heat flow, prevailing at a distance from centers of recent tectonic or magmatic activity, is 50 erg cm^{-2} s^{-1}. The difference between a chondritic heat flow and the observed heat flow can be explained either by a heat supply from the core or by an increase of the abundances [K], [Th] and [U]. For example, it could be imagined that radioactive elements have been eliminated from the liquid core and introduced in the mantle and in the crust. In this case, the chondritic abundances, multiplied by 1.47, lead to a heat flow of 59 erg cm^{-2} s^{-1}.

Wasserburg *et al.* (1964) analyzed the thermal balance with the ratio $[K]/[U] = 10^4$ and $[Th]/[U] = 3.7$, instead of a chondritic ratio $[K]/[U] \sim 7 \times 10^4$. Bieri *et al.* (1967) used this non-chondritic model to show that 99% of the helium outflow in the oceanic regions comes from the mantle. Later, MacDonald (1964) analyzed the non-chondritic model in detail. Using a uranium abundance 3 to 4 times higher than found in chondrites and taking $[K]/[U] = 10^4$ MacDonald (1964) found agreement between theory and the observed heat flow, provided that the initial temperature of the earth was at least 1275 K.

With a chondritic ratio $[Th]/[U] = 3.3$ (Morgan and Lovering, 1967) and a ratio $[K]/[U] = 10^4$, it can be shown that Equation (11) leads to a chondritic heat production of 5.014×10^{-8} erg g^{-1} s^{-1} for a uranium abundance $[U] = 2.30 \times 10^{-8}$ g g^{-1}. This implies that $[K] = 2.30 \times 10^{-4}$ g g^{-1} and $[Th] = 7.59 \times 10^{-8}$ g g^{-1}. Independently of the heat transport problems and the initial temperature of the Earth, Equation (11) clearly shows that the thermal balance alone cannot give unique abundances of potassium, thorium and uranium, and any estimate of the helium flux will reflect these uncertainties. Thus, two extreme cases can be discussed: a chondritic Earth with $[K]/[U] \sim 7\text{–}8 \times 10^4$ and an Earth with $[K]/[U] = 10^4$. Since the uranium and thorium abundances are smaller in a chondritic model, it is clear that this model will lead to the smallest helium flux, particularly because the degassing coefficient is smaller (see Figure 2).

The total helium content He_E^4 can be found using decay schemes similar to Equation (5). The result is

$$He_E^4 = \frac{6\lambda_{232} Th_0^{232}}{\delta - \lambda_{232}} (e^{-\lambda_{232} t} - e^{-\delta t}) + \frac{7\lambda_{235} U_0^{235}}{\delta - \lambda_{235}} (e^{-\lambda_{235} t} - e^{-\delta t}) + \\ + \frac{8\lambda_{238} U_0^{238}}{\delta - \lambda_{238}} (e^{-\lambda_{238} t} - e^{-\delta t}), \tag{12}$$

where Th_0^{232}, U_0^{235} and U_0^{235} are respectively the total amounts of thorium-232, of uranium-235 and of uranium-238 existing at the origin of the Earth ($t = 0$). The total amount of helium He_A^4 introduced into the atmosphere is then

$$\frac{dHe_A^4}{dt} = \delta He_E^4, \tag{13}$$

where the degassing coefficient δ is obtained from the argon-40 balance. The results for chondritic ($[K]/[U]=7\times10^4$) and for non-chondritic ($[K]/[U]=10^4$) models are presented on Figure 3. The non-chondritic model leads to a He^4 outflow of 3.8×10^6 atoms $cm^{-2}\ s^{-1}$, whereas the chondritic model gives an outflow of 6.8×10^5 atoms $cm^{-2}\ s^{-1}$ since the thorium and uranium abundances and the degassing coefficient are smaller. The dashed curves in Figure 3 give the helium production inside of the Earth. With the assumption that every He^4 atom produced in the earth escapes from the mantle and the crust, the non-chondritic model shows that production and outflow

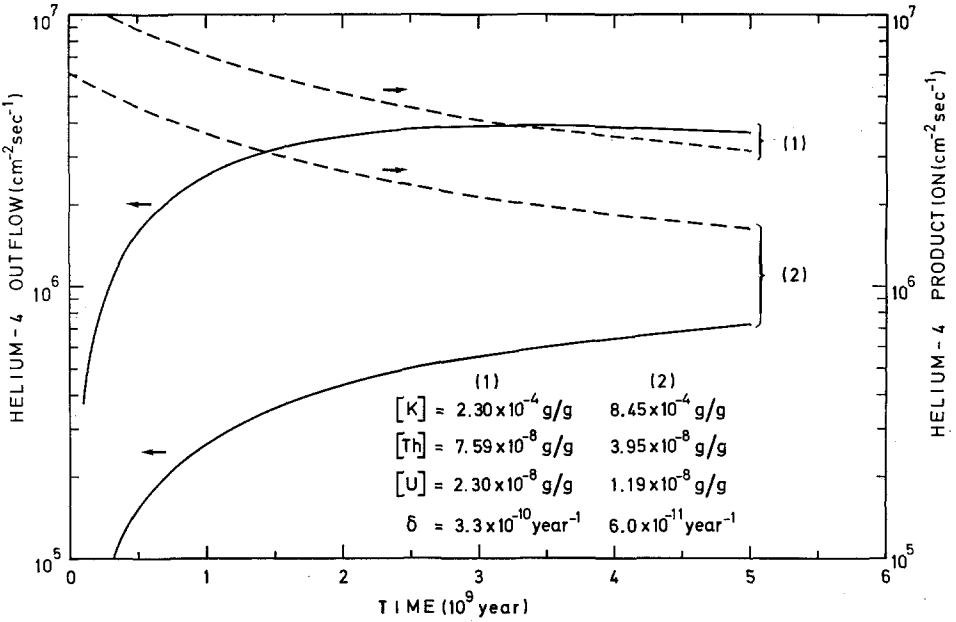

Fig. 3. Helium-4 outflow and production as a function of time. A non-chondritic model (1) and a chondritic model (2) are used in the computation.

are almost in balance at the present time. In a chondritic model, the He^4 production of 1.7×10^6 atoms $cm^{-2}\ s^{-1}$ is approximately a factor of 2.5 higher than the outflow of 6.8×10^5 atoms $cm^{-2}\ s^{-1}$. In the later case the helium outflow is still increasing with time, whereas in a non-chondritic model the He^4 outflow is currently decreasing slightly with time. In both models, the current heat flow produced by crust and mantle radioactivity is 40 erg $cm^{-2}\ s^{-1}$.

With the working hypothesis that $[K]/[U]=10^4$ and $[Th]/[U]=3.3$, it is possible to compute from Equation (11) the abundances of the radioactive materials which correspond to the observed global mean heat flow (63 erg $cm^{-2}\ s^{-1}$) and to the normal mean heat flow (50 erg $cm^{-2}\ s^{-1}$). The required abundances, given in Table II, are within the limits deduced by Larimer (1971) for uranium and thorium. The potassium abundances, however, are almost a factor of two higher. The corresponding degassing coefficients and the He^4 outflows are also given in Table II. A flux of 4.3×10^6 atoms

TABLE II

Abundances, degassing coefficients and helium-4 outflow

Heat flow (erg cm^{-2} s^{-1})	63	50
[K] (g g^{-1})	3.63×10^{-4}	2.88×10^{-4}
[Th] (g g^{-1})	1.20×10^{-7}	9.51×10^{-8}
[U] (g g^{-1})	3.63×10^{-8}	2.88×10^{-8}
δ (yr^{-1})	1.65×10^{-10}	2.29×10^{-10}
$F(He^4)$ (cm^{-2} s^{-1})	4.3×10^{6}	4.1×10^{6}

cm^{-2} s^{-1} is the maximum value compatible with the heat flow measured at ground level. Within the framework of the different models which have been discussed, the helium-4 flux could range between 6.8×10^5 and 4.3×10^6 atoms cm^{-2} s^{-1}. This uncertainty range is slightly smaller than that suggested by MacDonald (1963).

The experimental determination of the He^4 outflow at ground level is not an easy task since, with a mixing ratio of 5.24×10^{-6}, a flux of $4\ 4 \times 10^6$ atoms cm^{-2} s^{-1} implies an extremely small transport velocity of 3×10^{-8} cm s^{-1}. The experimental data presently available come from He^4 concentration measurements in the oceans. These data indicate an He^4 excess with relation to the other rare gases (Bieri *et al.*, 1964, 1966; Clarke *et al.* 1969, 1970; Craig and Clarke, 1970; Craig and Weiss, 1971; Bieri, 1971; Jenkins *et al.*, 1972; Bieri and Koide, 1972). Although the interpretations of this type of measurement are not always in agreement, it has been possible, however,

TABLE III

Helium flux in the deep ocean

He^4 (cm^{-2} s^{-1})	He^3 (cm^{-2} s^{-1})	Reference
2×10^6	–	Bieri *et al.* (1964)
–	2	Clarke *et al.* (1969)
$(7.7 \pm 3) \times 10^5$	5.5 ± 2	Craig and Clarke (1970)
$(2 \pm 1) \times 10^6$	–	Bieri and Koide (1972)

to deduce the fluxes given in Table III. The various difficulties involved in these measurements have been discussed by Bieri and Koide (1972). In particular, it should be noted that the fluxes deduced from concentration gradients require the knowledge of an oceanic eddy diffusion coefficient. It appears however, that the He^4 fluxes of Table III are roughly in agreement with the values previously deduced from the radioactive decay of uranium and thorium. With our present knowledge it is difficult to choose between fluxes lying between 7×10^5 and 4×10^6 atoms cm^{-2} s^{-1}. Since the non-chondritic model of the Earth seems now to be acceptable, one can attempt to adopt a mean He^4 flux of $(2.5 \pm 1.5) \times 10^6$ atoms cm^{-2} s^{-1}. The smallest values of Table III cannot be excluded since a geographical variation may be possible. Such a variation has already been observed for helium-3 by Jenkins *et al.* (1972) where it was found that the He^3 excess in the Atlantic ocean is much smaller than the excess observed by Clarke *et al.* (1970) in the Pacific Ocean.

3. Helium-3 Production Rate

The isotope He^3 never becomes a major component of the terrestrial atmosphere, but a study of its behavior is very useful to analyse the consistency of the proposed escape mechanisms for He^4 which will be discussed in Section 6.

Only a few ground level measurements are available for the He^3 isotopic abundance in the Earth's atmosphere (Aldrich and Nier, 1948; Coon, 1949). The normally adopted isotopic abundance at ground level is $He^3/He^4 = 1.25 \times 10^{-6}$, leading to a mixing ratio of 6.55×10^{-12}. The He^3 isotopic abundance is however highly variable in nature. Cameron (1968), for example, proposed a solar system ratio $He^3/He^4 \sim 3 \times 10^{-4}$, based on the ratio usually found in trapped helium from meteorites. Nevertheless, great range in isotopic composition is found in meteorites (Heymann, 1971) and the ratio He^3/He^4 can vary by three orders of magnitude. Such isotopic variations can, however, be explained in terms of mixtures of three components present in different proportions: a cosmic-ray component, a radiogenic component and a trapped component. For gas-rich meteorites the trapped component ratio is $He^3/He^4 \sim 3 \times 10^{-4}$ (Signer and Suess, 1963; Heymann, 1971). In the Sun the isotopic abundance ratio He^3/He^4 may be deduced from the chromospheric absorption line at 10830 Å. The value of 2×10^{-4} proposed by Goldberg (1962) has been reduced to less than 10^{-4} by Namba (1965). We can immediately note, however, that those values are two orders of magnitude higher than the values observed at ground level in the terrestrial atmosphere.

There is no direct radioactive decay process which leads to He^3 from terrestrial elements. A very small production through secondary nuclear reactions can, however, explain the ratio $He^3/He^4 \sim 10^{-7}$ observed in natural gas wells (Aldrich and Nier, 1948). The different sources which are usually considered for the production of atmospheric He^3 are: cosmic ray interactions yielding He^3 directly; galactic cosmic ray interactions followed by tritium β decay; solar cosmic ray interactions; and meteorites and cosmic dust. These processes, discussed in detail by Johnson and Axford (1969), lead to a production of the order of 1 atom $cm^{-2}\ s^{-1}$. In their analysis of the atmospheric He^3 budget, Johnson and Axford (1969) suggested a new source of He^3 arising from an auroral precipitation of solar wind He^3 ions of 4 particules $cm^{-2}\ s^{-1}$. Thus the total atmospheric production rate of He^3 is of the order of 5 atoms $cm^{-2}\ s^{-1}$. By comparing the accretion rates to the loss rates, Axford (1970) concluded that this auroral mechanism is only effective for He^3; i.e. the budgets for H^1, H^2 and He^4 are not appreciably affected.

Recently Clarke *et al.* (1969) and Craig and Clarke (1970) deduced the presence of He^3 fluxes from concentration measurements in the deep ocean (see Table III). With a He^3 flux of 5 atoms $cm^{-2}\ s^{-1}$, the flux ratio $F(He^3)/F(He^4) = 2 \times 10^{-6}$; i.e. a value of the same order of magnitude as the ground level isotopic ratio. The origin of this additional He^3 flux in the ocean is not completely clear. Clarke *et al.* (1969) conclude that the excess He^3 is due to leakage into the ocean water of a remnant of the Earth's primordial He^3. In contrast, Fairhall (1969) attributes a large fraction

of the excess He^3 in the deep sea to the decay of natural tritium. Craig and Clarke (1970), however, pointed out that Fairhall (1969) may have used a tritium concentration which is too large and that the tritium decay can lead only to a flux of 0.25 at cm^{-2} s^{-1}. More recently Craig and Weiss (1971), Bieri (1971) and Jenkins *et al.* (1972) concluded that an important fraction of the helium excess can be accounted for through the injection of air into seawater. When all the present uncertainties are taken into account, it appears that the helium-3 influx into the atmosphere is approximately (7.5 ± 2.5) atoms cm^{-2} s^{-1}. These values will have to be compared with the escape flux discussed later.

4. Helium in the Thermosphere

4.1. Observations

Information on the helium-4 distribution in the upper atmosphere is presently available from three different techniques: infrared and ultraviolet optical observations, satellite drag data and mass spectrometric measurements. Due to its very low abundance, no direct data are presently available for the helium-3 isotope.

The presence of helium above 500 km was experimentally inferred from infrared observation at 10830 Å during the great aurora of February 10–11, 1958 (see Shefov, 1961). The $2\ ^3S$–$2\ ^3P$ transition has been regularly observed in the polar region during twilight and Shefov (1961) deduced a concentration of 1.5×10^6 cm^{-3} at 500 km, a value which is in fair agreement with more recent observations. Christensen *et al.* (1971) presented a detailed analysis of this type of measurements whereas Brandt *et al.* (1965) detected also the $2\ ^3S$–$3\ ^3P$ transition at 3888 Å. In the ultraviolet region, the 584 Å emission corresponds the a $1\ ^1S$–$2\ ^1P$ transition of neutral helium and it is now observed by rockets above the main absorbing atmosphere.

Ionized helium has also been detected from its 304 Å $1\ ^2S$–$2\ ^2P$ emission. Meier and Weller (1972) have analyzed the extreme ultraviolet data by calculating the full resonant multi-scattering of 584 Å solar radiation and by using a single-scattering theory for the 304 Å emission of ionized helium. Since a complete discussion of the helium optical emissions has been given recently by Mange (1973) a detailed account of the results is not needed here. It should be noted, however, that according to Carlson (1972), airglow measurements near 304 Å can contain a significant contribution from doubly ionized atomic oxygen which has a resonance line at 303.799 Å.

Nicolet (1961) showed that helium was needed to explain the atmospheric drag experienced by the satellite Echo 1, since both atomic oxygen and hydrogen were unable to provide a consistent explanation of the orbital varitions. The analysis of drag data of several satellites like Echo 2 (Cook, 1967), Explorer 9, 14, 19 (Keating and Prior, 1968; Keating *et al.*, 1970) showed the existence of an increase in the total density at high latitudes for winter conditions. This effect is attributed to a winter helium bulge and Keating *et al.* (1970) have deduced that the helium density over the winter polar thermosphere is approximately three to four times higher than over the summer pole.

The first *in situ* observation made by a mass spectrometer on Explorer 17 (Reber and Nicolet, 1965) indicated a latitudinal variation of the helium concentration. Further measurements were made on Explorer 32 (Reber *et al.*, 1968) and the recent data from OgO 6 show a larger amplitude for the winter helium bulge (Reber *et al.*, 1971). Whereas the drag data (Keating *et al.*, 1970) lead to a variation of approximately a factor of four between summer and winter polar regions, the mass spectrometric data (Reber *et al.*, 1971) show an amplitude of the order of a factor of ten. Several rocket measurements of helium (Kasprzak *et al.*, 1968; Krankowsky *et al.*, 1968; Müller and Hartmann, 1969; Bitterberg *et al.*, 1970; Hickman and Nier, 1972) are available for the atmospheric regions between 120 km and 200 km altitude. The

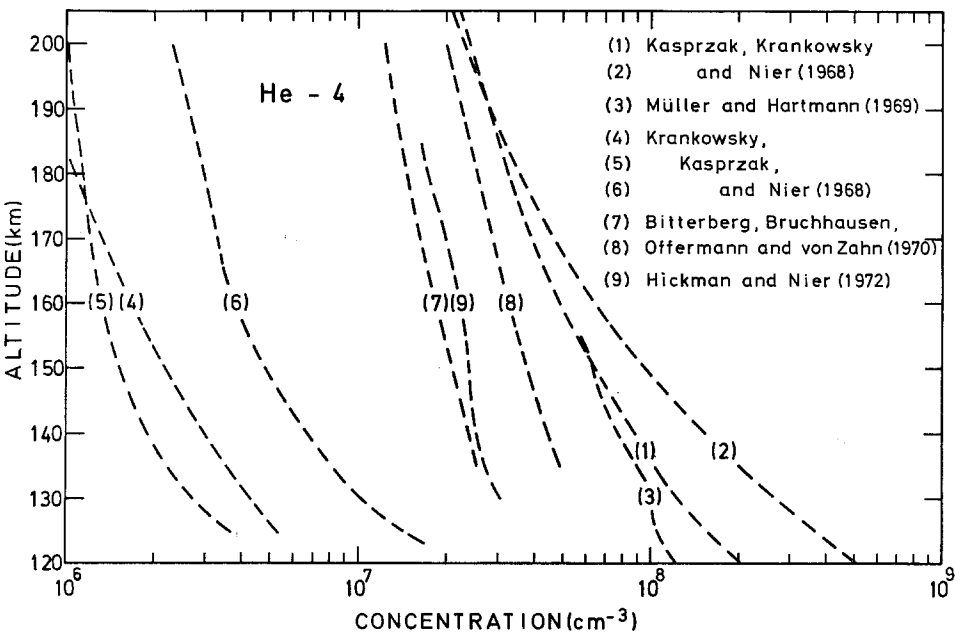

Fig. 4. Mass spectrometric observations of the helium-4 distribution in the thermosphere.

TABLE IV

Rocket mass spectrometric measurements of helium

N° Launching site	Date	Zone time	Reference
(1) White Sands (32°24 N, 106°21 W)	30 Nov., 1966	04.45	Kasprzak *et al.* (1968)
(2) White Sands (32°24 N, 106°21 W)	2 Dec., 1966	14.09	Kasprzak *et al.* (1968)
(3) Fort Churchill (58°44 N, 93°49 W)	12 Dec., 1966	13.05	Müller and Hartman (1969)
(4) White Sands (32°24 N, 106°21 W)	21 June, 1967	12.49	Krankowsky *et al.* (1968)
(5) White Sands (32°24 N, 106°21 W)	20 July, 1967	02.00	Krankowsky *et al.* (1968)
(6) White Sands (32°24 N, 106°21 W)	20 July, 1967	12.24	Krankowsky *et al.* (1968)
(7) Salto di Quirra (40° N, 9°30 E)	4 Oct., 1967	14.23	Bitterberg *et al.* (1970)
(8) Salto di Quirra (40° N, 9°30 E)	10 Oct., 1967	15.33	Bitterberg *et al.* (1970)
(9) Fort Churchill (58°44 N, 93°49 W)	4 Feb., 1969	08.35	Hickman and Nier (1972)

concentrations are shown on Figure 4 while the date, time and location of each rocket launch are given in Table IV.

It is clear from Figure 4 that a He^4 concentration variation greater than an order of magnitude has been observed in a height range where helium is still a minor component. Such a variation is not present for the other major atmospheric constituents (O, O_2, N_2). In addition, atomic hydrogen, another minor component, shows variations which are less than a factor of three. Unfortunately, there exist no helium measurements below 120 km, which could give some insight into the physical mechanism responsible for such a behavior. Noble gases from air samples collected between 43 and 63 km confirm expectations that the atmosphere is well mixed up to, and within, the lower mesosphere (Bieri *et al.*, 1970). In the first theoretical computations of vertical helium distributions, Kockarts and Nicolet (1962, 1963) assumed a perfect mixing up to 105 km where diffusive equilibrium was assumed to begin. Such a level is often called the turbopause, but it corresponds actually to an extended region where there is a transition from mixing to molecular diffusion. The major problem is, however, to explain how a helium-4 mixing ratio of 5.24×10^{-6} in the homosphere can increase by an order of magnitude between approximately 90 km and 120 km altitude. The various mechanisms which have been proposed to explain this altitude variation will now be discussed.

4.2. Transport processes

Since helium-4 is produced inside of the Earth and is furthermore chemically inert, production and loss terms can be neglected in the thermosphere. For helium-3 it is possible to assume that the production and the influx in the homosphere leads to a mixing distribution. Therefore a constant mixing ratio is adopted at the lower boundary where transport processes start. The helium continuity equation is

$$\frac{\partial n_1}{\partial t} + \operatorname{div}(n_1 \mathbf{w}_1) = 0, \tag{14}$$

where n_1 is the He^4 or He^3 concentration, t is the time and $\mathbf{w}_1$ is the transport velocity of He^4 or He^3. For steady state conditions and with lateral symmetry, Equation (14) leads to the condition

$$F(r_0)\, r_0^2 = F(r)\, r^2, \tag{15}$$

where $F(r_0)$ and $F(r)$ are respectively the radial fluxes at the geocentric distances r_0 and r. Generally, the transport velocity $\mathbf{w}_1$ arises from three effects and the transport flux $\mathbf{F}$ can be written

$$\mathbf{F} = n_1 \mathbf{w}_1 = n_1 (\mathbf{w}_D + \mathbf{w}_E + \mathbf{u}), \tag{16}$$

where $\mathbf{w}_D$ is the molecular diffusion velocity, $\mathbf{w}_E$ is the eddy diffusion velocity and $\mathbf{u}$ is the velocity arising from any fluctuations, winds or circulation systems. Theoretical expressions are available only for the first two terms of Equation (16).

With the general diffusion equation of Chapman and Cowling (1960) it is possible to show (Mange, 1961; Nicolet, 1968; Kockarts, 1971) that the vertical component of the molecular diffusion velocity for a minor constituent at height z is given by

$$w_D = -D\left(\frac{1}{n_1}\frac{dn_1}{dz} + \frac{1}{H_1} + \frac{1+\alpha}{T}\frac{dT}{dz}\right), \tag{17}$$

where D is the molecular diffusion coefficient, α is the thermal diffusion factor, T is the temperature and H_1 is the scale height $kT/m_1 g$.

Following Lettau (1951), the vertical eddy diffusion velocity can be written

$$w_E = -K\left(\frac{1}{n_1}\frac{dn_1}{dz} + \frac{1}{H} + \frac{1}{T}\frac{dT}{dz}\right), \tag{18}$$

where K is the eddy diffusion coefficient and H is the atmospheric scale height kT/mg.

Expressions for $\mathbf{u}$ varies according to the meaning given to this term. Integration of the vertical component of Equation (16) with (17) and (18) leads to the following expression

$$n_1(z) = n_{eq}\left[1 - \int_{z_0}^{z} \frac{F}{D(1+\Lambda)\, n_{eq}}\, dz\right], \tag{19}$$

where $\Lambda \equiv K/D$, z_0 is the lower boundary altitude and n_{eq} is the zero flow solution obtained from (16) with the condition $F=0$. Expressions similar to (19) have been obtained by Kasprzak (1969), Donahue (1969) and Kockarts (1971; 1972a). From Equation (19) it is clear that an upwards flux ($F>0$) will always lead to helium concentrations $n_1(z)$ smaller than those given by the zero flow distribution

$$n_{eq}(z)/n_1(z_0) = (T_0/T) \times$$
$$\times \exp -\left[\int_{z_0}^{z}\left(\frac{1}{H_1} + \frac{\Lambda}{H} - \frac{u}{D}\right)(1+\Lambda)^{-1}\, dz + \int_{z_0}^{z} \alpha(1+\Lambda)^{-1}\frac{dT}{T}\right]. \tag{20}$$

The continuity condition (15) implies that the knowledge of the flux at one height is sufficient to determine the flux at any other height. When the vertical velocity w_1 increases more rapidly than $1/n_1$, a lateral inflow is necessary to maintain the continuity requirements. A lateral outflow occurs however when w_1 increases less rapidly than $1/n_1$. The idea of lateral flows has been used by Johnson and Gottlieb (1970), by Reber (1971) and by Reber and Hays (1973) to deduce a meridional circulation system compatible with the observed winter bulge. An upward wind introduced over the summer pole and a downward wind over the winter pole is found to lead to an increase of the helium concentration over the winter pole. The wind field consistent with the OgO-6 measurements is characterized by vertical velocities of 2 to 3 m s^{-1} above 200 km and horizontal velocities of 100 to 200 m s^{-1} at the equator (Reber, 1971). These are within a factor of two of the amplitudes deduced by Johnson and

Gottlieb (1970). The altitude of the circulation cell introduced by Reber (1971) is, however, approximately 100 km higher than the meridional circulation proposed by Johnson and Gottlieb (1970). In Reber's calculations, the eddy diffusion coefficient is assumed to be invariant with latitude. It is also clear from Equations (19) and (20) that sufficiently strong winds will distort the concentration profile and even change the sign of the concentration gradient.

The first attempt to explain the measured helium distribution indicated in Figure 4 was made by Kasprzak (1969) who used Equations (19) and (20) with $\Lambda=0$ and $u=0$ implying the absence of eddy diffusion and winds. The flux, F, in (19) was adjusted to fit the observed distributions. Upward fluxes between 2×10^{8} and 3×10^{10} cm^{-2} s^{-1} are obtained in this way. Such fluxes are greater than the surface He-4 production flux and they are also higher than the maximum flow which can be supported by diffusion (see later discussion).

Internal gravity waves create large atmospheric fluctuations. Hodges (1970) obtained an expression identical to (16) omitting the eddy diffusion term and taking μ to be the vertical velocity resulting from the correlation of fluctuating atmospheric parameters. By approximating internal gravity waves by a typical monochromatic wave, Hodges (1970) obtained an expression for u which is negative for helium. This implies a downward transport. The contradiction is not real, however, since the fluctuations introduced by Hodges (1970) tend to create a departure from an initial diffusive equilibrium. Equation (20) actually shows that with $\Lambda=0$, a negative value of μ leads to a sharper decrease of the zero flow distribution and it was implicitely assumed by Hodges (1970) that the net flow F in (19) is negligible. Owing to the approximations which were made, Hodges (1970) recognized that quantitative comparison with measurements was not practical. Non linear effects of wave-induced atmospheric fluctuations can however play a role in the u term of Equation (16).

Another approach of the problem of the altitude distribution of helium is directly based on Equations (19) and (20) in which the velocity u is assumed to be zero (Kockarts, 1971; 1972a). Since the molecular diffusion coefficient is rather wellknown, the eddy diffusion coefficient K can be taken as a parameter in Equations (19) and (20). Figure 5 taken from (Kockarts, 1972a) gives the eddy diffusion coefficient necessary to explain the observations of Reber *et al.* (1971) as a function of latitude. It is seen that the eddy diffusion coefficient should decrease by more than a order of magnitude between summer and winter hemispheres, if the entire helium bulge results from such a process. In support of this idea according to the theory presented by Johnson and Gottlieb (1970), the eddy diffusion coefficient is much smaller over the winter polar region, since less heat has to be transported downwards. In contrast, Zimmerman *et al.* (1972) showed that the winter polar mesosphere is more turbulent than the summer polar mesosphere below 90 km. The latitudinal variation of the eddy diffusion coefficient on Figure 5 applies, however, to the region between 90 km and 120 km, where almost no experimental data are available (see however Lloyd *et al.*, 1972). Colegrove *et al.* (1965) showed that the ratio $n(O)/n(O_2)$ is a function of the eddy diffusion coefficient. Therefore, a latitudinal variation of K would imply a latitudinal variation

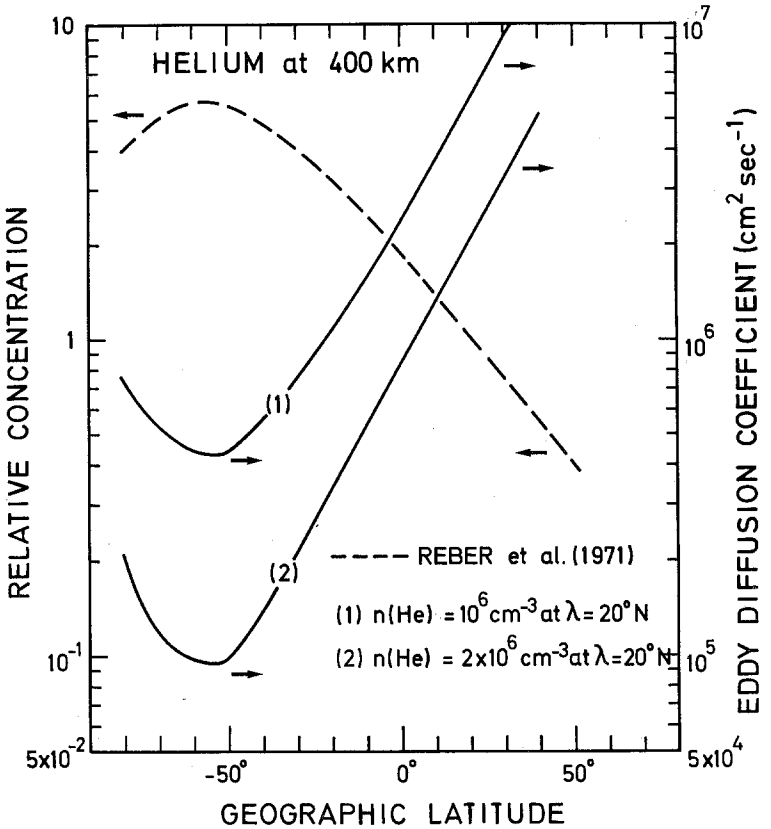

Fig. 5. Latitudinal variation of a height independant eddy diffusion required to explain observations of the winter helium bulge. The two curves correspond to different normalizations of the concentration at $\lambda = 20°$ N. This figure is taken from Kockarts (1972a).

of atomic oxygen. Such a variation, however, cannot be as important as for He^4, since the photodissociation of O_2 is drastically recuced over the winter polar region. Furthermore, the effect of eddy diffusion becomes smaller when the mass of a constituent becomes closer to the mean molecular mass.

In order to obtain consistency between drag data and OGO-6 measurements, Keating *et al.* (1972) showed that it is necessary to adopt an atomic oxygen maximum at *low* latitude in the winter hemisphere rather than assuming a constant concentration with latitude. This maximum occurs at low latitude since the O_2 photodissociation is stronger at low latitude during the winter. It is however necessary to investigate how eddy diffusion affects other light constituents. The effects on atomic hydrogen (Kockarts, 1972a) and on deuterium (Kockarts, 1972b) have already been discussed. The case of helium-3 and argon-40 will now be investigated in some detail.

4.3. Diffusion velocities and vertical profiles

The concept of a maximum diffusion flux, introduced by Mange (1955, 1961), has

been applied many times to aeronomical problems. When a minor constituent diffuses through the atmosphere, its diffusion velocity is given by Equation (17). If this constituent is initially completely mixed with the atmosphere, the concentration gradient in (17) is identical with the concentration gradient of the major species. The maximum molecular diffusion velocity obtained from (17) is then

$$w_D(\mathrm{MAX}) = \frac{D}{H}\left(1 - \frac{H}{H_1} - \frac{\alpha H}{T}\frac{\mathrm{d}T}{\mathrm{d}z}\right). \tag{21}$$

This velocity is upwards for light constituents ($m_1 < m$) and downwards for heavy constituents ($m_1 > m$). Table V gives the maximum molecular diffusion velocity for He^3, He^4 and Ar^{40}. The molecular diffusion coefficient used in the computations is given by

$$D = 1.5 \times 10^{18}\left(\frac{1}{M_1} + \frac{1}{M}\right)^{1/2}\frac{T^{1/2}}{n}\ (\mathrm{cm^2\ s^{-1}}), \tag{22}$$

where M_1 and M are respectively the minor constituent mass and the atmospheric mean molecular mass expressed in atomic mass units, n is the total atmospheric concentration. The thermal diffusion factor is -0.38 for He^3 and He^4 and can be

TABLE V

Maximum molecular diffusion velocities

z(km)	T(K)	H(km)	$n(\mathrm{cm^{-3}})$	$w(He^4)$ (cm s^{-1})	$w(He^3)$ (cm s^{-1})	w(Ar) (cm s^{-1})
85	160.3	4.82	1.77×10^{14}	1.08×10^{-1}	1.27×10^{-1}	-2.12×10^{-2}
90	176.7	5.34	6.01×10^{13}	3.01×10^{-1}	3.54×10^{-1}	-5.91×10^{-2}
95	193.0	5.85	2.26×10^{13}	7.63×10^{-1}	8.99×10^{-1}	-1.50×10^{-1}
100	209.2	6.41	9.35×10^{12}	1.78×10^{0}	2.09×10^{0}	-3.58×10^{-1}
105	230.9	7.24	4.01×10^{12}	3.95×10^{0}	4.65×10^{0}	-8.48×10^{-1}
110	261.9	8.42	1.97×10^{12}	7.35×10^{0}	8.67×10^{0}	-1.72×10^{0}
115	293.0	9.63	1.01×10^{12}	1.33×10^{1}	1.56×10^{0}	-3.32×10^{0}
120	324.0	10.87	5.42×10^{11}	2.30×10^{1}	2.72×10^{0}	-6.14×10^{0}

neglected for argon. Its effect on the vertical helium distribution is discussed by Kockarts (1963). The values quoted in Table V apply to the case when the constituent is initially in perfect mixing. The real diffusion velocity is always smaller since there is a tendency towards diffusive equilibrium where $w_D = 0$.

When a perturbation occurs in the atmosphere, departures from diffusive equilibrium can occur and the minor constituent has a tendency towards perfect mixing. The maximum eddy diffusion velocity, obtained in the same way from Equation (18), is then

$$w_E(\mathrm{MAX}) = -\frac{K}{H}\left(1 - \frac{H}{H_1} - \frac{\alpha H}{T}\frac{\mathrm{d}T}{\mathrm{d}z}\right). \tag{23}$$

This velocity has a sign opposite to the maximum molecular diffusion velocity. When $D = K$, the absolute values of these velocities are identical.

With the values of Table V and the abundances of He^3, He^4 and Ar^{40}, the maximum molecular diffusion flows at 90 km are respectively

$$F_M(He^3) = 1.4 \times 10^2 \text{ cm}^{-2} \text{ s}^{-1} \tag{24}$$

$$F_M(He^4) = 9.5 \times 10^7 \text{ cm}^{-2} \text{ s}^{-1} \tag{25}$$

$$F_M(Ar^{40}) = -3.3 \times 10^{10} \text{ cm}^{-2} \text{ s}^{-1}. \tag{26}$$

When the real flow F is negligible compared to the maximum flow, Equation (19) reduces practically to the zero flow distribution (20). This is actually the case for He^4, since the outgassing flow of He^4 is $(2.5 \pm 1.5) \times 10^6$ cm^{-2} s^{-1}. In order to satisfy the continuity equation, an influx at the lower boundary must be balanced by an outflux at the top of the atmosphere. Thermal escape is a valid candidate. Such a situation is known to occur for atomic hydrogen, but for helium-4 thermal escape is not sufficiently effective. For helium-3 the situation depends upon temperature, as illustrated Figure 6. For temperatures less than 1500K, the He^3 escape flux is not strong enough to affect the vertical distribution and the concentration is controlled by the relative importance of K and D. For temperatures higher than 1500K, the effect of eddy diffusion decreases. For helium-4 the escape flux has a negligible effect upon the density profile. In these computations K is constant with height and the upper and lower boundaries are respectively at 1000 km and 90 km. Although the eddy diffusion coefficient is actually variable with height above 90 km (Johnson and Gottlieb, 1970;

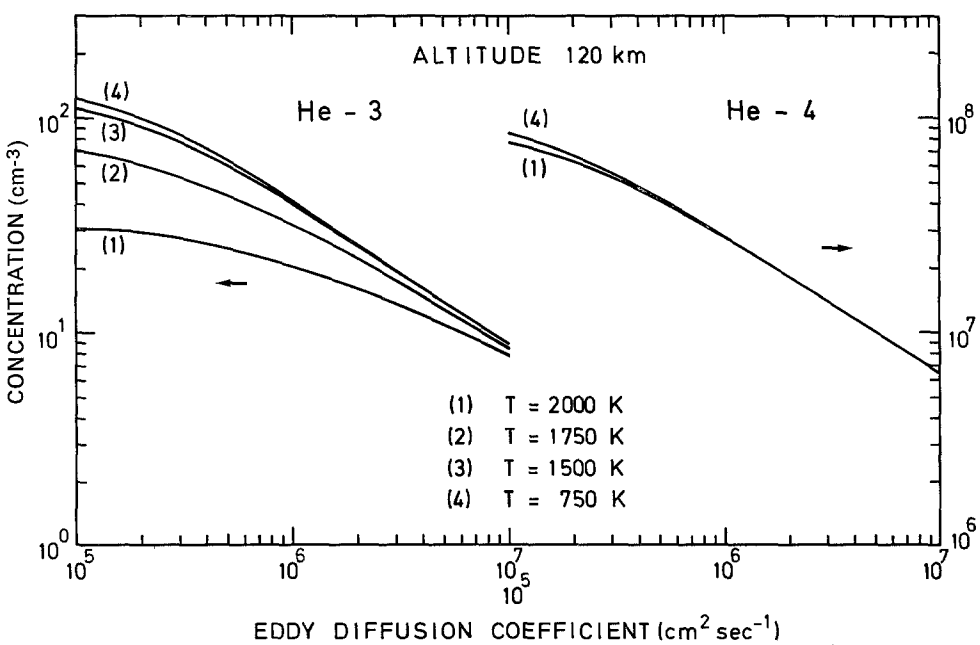

Fig. 6. Comparison between the reaction of helium-3 and helium-4 to a change of the eddy diffusion coefficient.

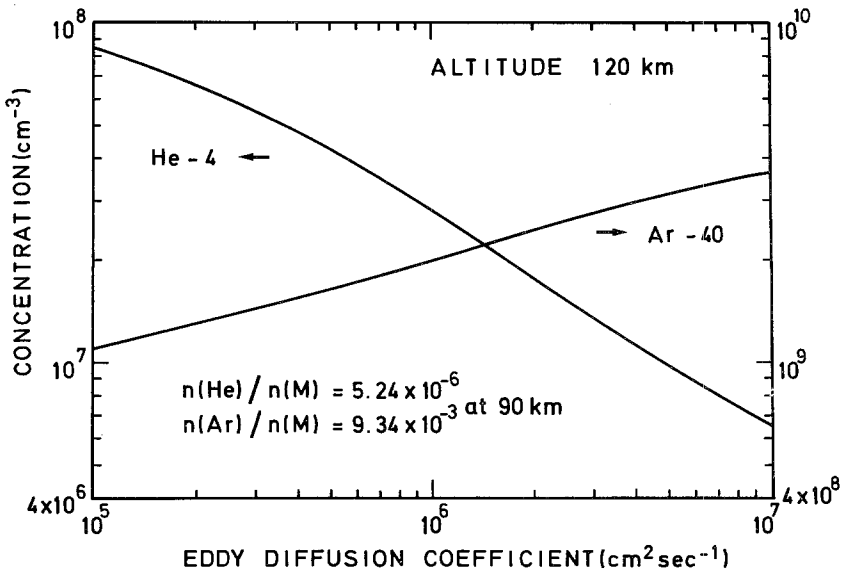

Fig. 7. Comparison between the reaction of argon-40 and helium-4 to a change of the eddy diffusion coefficient.

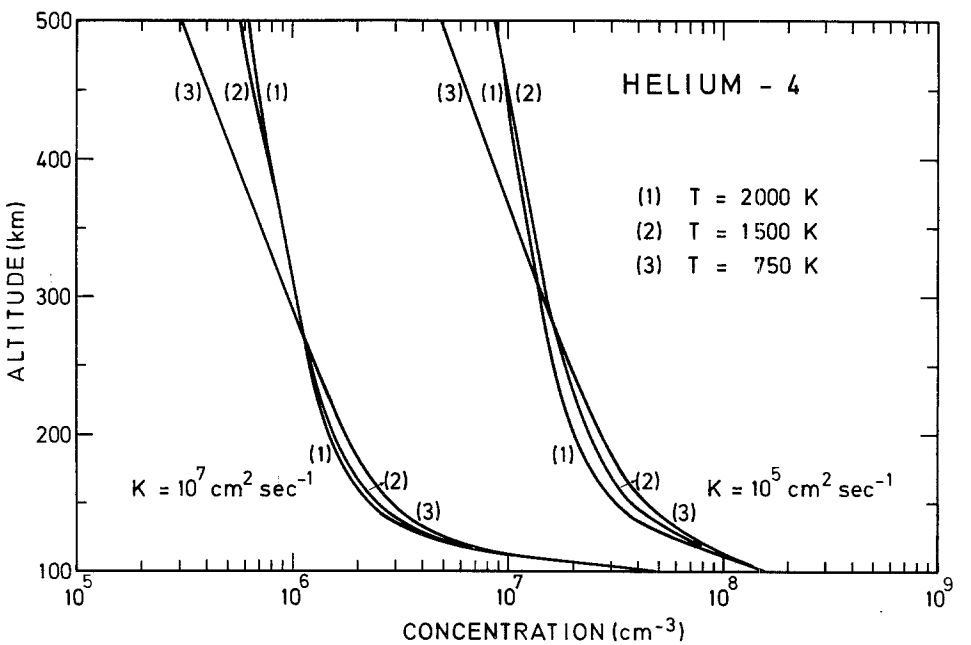

Fig. 8. Helium-4 vertical distributions for two extreme values of the eddy diffusion coefficient. The variation with temperature is almost negligible below 300 km.

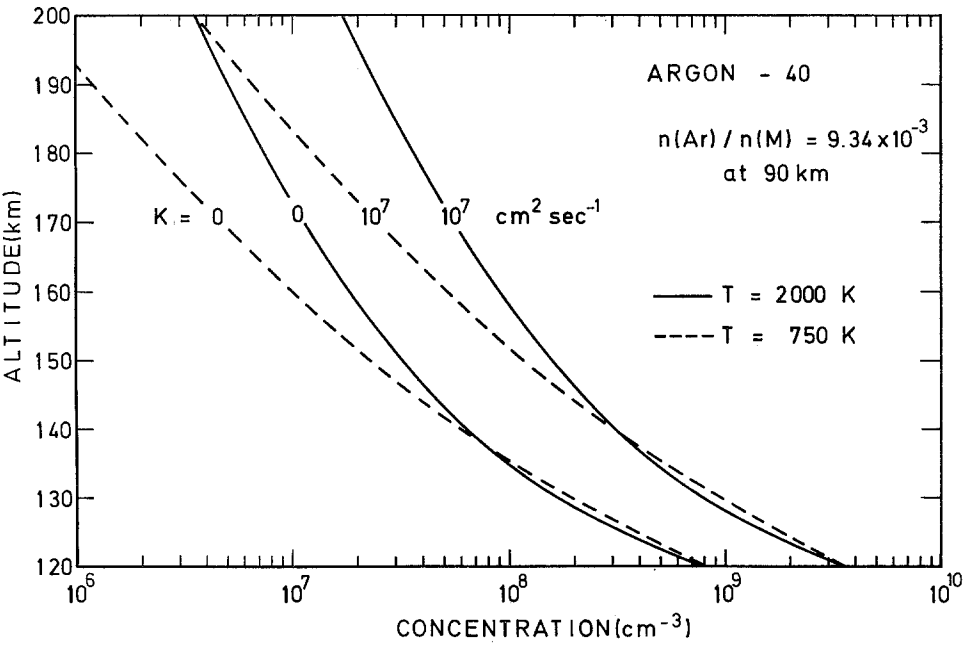

Fig. 9. Argon-40 vertical distributions for $K=0$ and $K=10^7$ cm^2 s^{-1}. The variation with the thermopause temperature is more important than in Figure 8.

Keneshea and Zimmerman, 1970), constant values have been used just to show the nature of the effect. Height dependent coefficients lead to similar results (Kockarts, 1972a).

Figure 7 indicates how Ar^{40} reacts to a change of the eddy diffusion coefficient. An increase of K leads now to an increase of the argon concentration. This situation is easily understood by comparing the sign of w_D for Ar^{40} and He^4. Moreover the variation of the Ar^{40} concentration as a function of K is less than that for He^4.

Finally Figures 8 and 9 give examples of possible vertical distributions for helium and argon when the wind term u is neglected in Equation (20). From Figure 8 it is seen how changes in the eddy diffusion can lead to large variations in the helium concentrations. Such variations can be compared with the observed distributions given by Figure 4. Furthermore, it is clear that the thermospheric temperature distribution has a negligible effect on thermospheric helium. Actually, Figure 9 shows that argon is more sensitive to the temperature. Extreme values of the eddy diffusion coefficient lead only to a variation of approximately a factor of four in the argon concentration at 120 km height. The argon measurements listed in Table IV fall all between the extreme curves of Figure 9. The average value of 5×10^7 cm^{-3} proposed by von Zahn (1970) at 150 km corresponds to a constant eddy diffusion coefficient of the order of 10^6 cm^2 s^{-1}.

From the previous discussion it appears that eddy diffusion and wind systems can

provide an explanation for the observed helium distribution in the thermosphere as well as for the observed winter helium bulge. It is difficult, however, to determine which effect is predominant, since no direct wind or eddy diffusion observations are presently available. Both aspects may be complementary and appear only as over-simplified representations of a complex natural phenomenon.

5. Ionized Helium

Since helium-4 becomes a major atmospheric constituent above 750 km, it is necessary to discuss the ionization processes which can lead to helium ions in the topside ionosphere. Mange (1960) showed how a minor ion concentration can increase with height under electrostatic equilibrium conditions. Bates and Patterson (1962) and Kockarts and Nicolet (1963) analyzed the He^+ distributions in the topside ionosphere when production and loss terms are involved at the lower boundary. Bauer (1966) showed that He^+ ions do not become a dominant topside ion at low solar activity, whereas they can play a significant role during high solar activity. The results of an ion probe

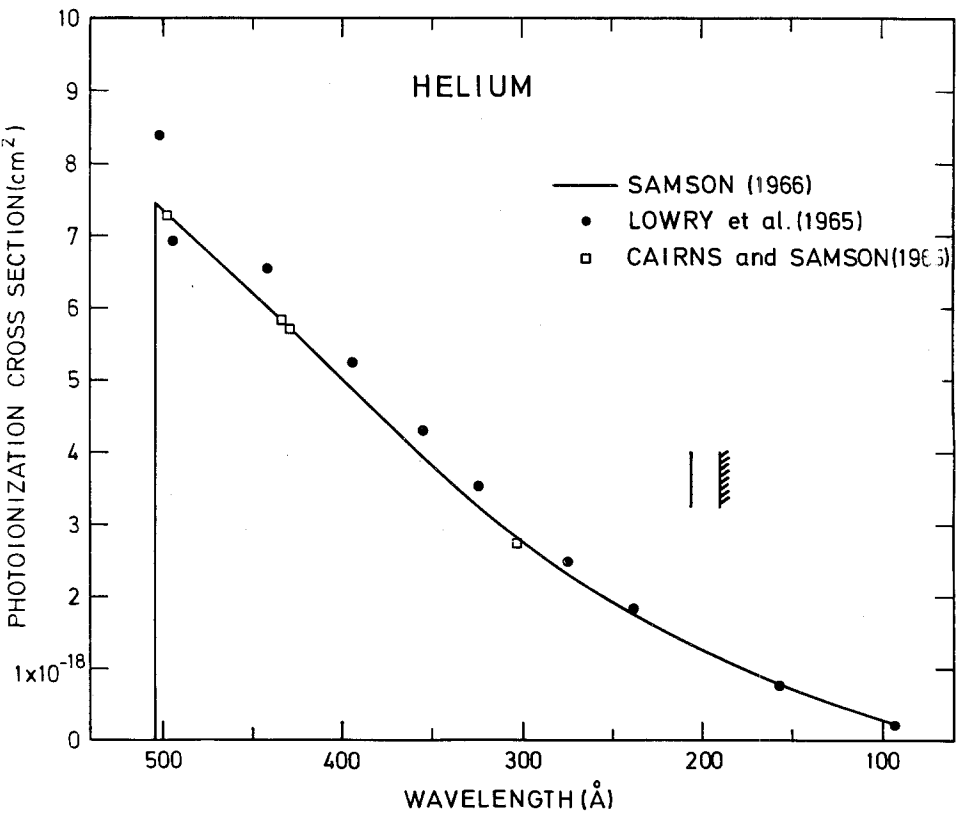

Fig. 10. Helium-4 photoionization cross section between 500 Å and 100 Å. The vertical lines indicate the position of a resonance series.

experiment (Hanson, 1962) and of retarding potential experiments on Explorer-8 (Bourdeau *et al.*, 1962) were explained by an important contribution of He^+ ions. A He^+ concentration of 7×10^3 cm^{-3} at 575 km was detected by an ion mass spectrometer (Taylor *et al.* 1963) in October 1961, when the helium ion concentration was higher than the hydrogen ion concentration between 400 km and 950 km. Later satellite measurements (Taylor, 1971; 1972) have a general tendency to indicate that He^+ is now less abundant than H^+ in the topside ionosphere although sometimes, usually at the plasmapause He^+ is more abundant than H^+ (Taylor, 1971). The global distribution of He^+ is rather complex owing to the solar, geomagnetic, and seasonal control of the topside ionosphere. Recently Taylor (1972) discussed the morphology of the light ion trough, i.e. the sharp decrease of the H^+ and He^+ concentration at dipole latitudes greater than 60°. In contrast to the trough in electron density at night, (which is affected by a number of counteracting factors) the light ion trough persists during both day and night and appears to be associated with magnetospheric convection and polar wind flows of H^+ and He^+ (see Banks, 1972).

The theoretical investigation of helium ions in the upper ionosphere requires a knowledge of the ionization processes and the subsequent ionic relactions. Helium-4 is photoionized by solar radiation with wavelength $\lambda \leqslant 504.26$ Å (24.69 eV). This process is effective only above the F-layer, where absorption by atomic oxygen (leading to O^+) can be neglected. The helium ionization cross section, reviewed by Samson (1966), is given on Figure 10 extending from the ionization limit down to 100 Å. The squares correspond to values measured by Cairns and Samson (1965) at intense solar emission lines. Although the ionization cross section given by Samson (1966) at 504 Å is approximately 10% lower than the value deduced by Lowry *et al.* (1965), there is relatively good agreement between experimental and theoretical results in the 500–100 Å range. The vertical lines indicate the position of a resonance line series observed by Madden and Codling (1965). This series is associated with transitions from the ground state to two-electron excitation states of neutral helium. Madden and Codling (1965) conclude that this series converges to the $n=2$ states of He^+ around 190 Å. The absorption cross section at the most intense resonance line (206.21 Å) reaches 10^{-17} cm^2, i.e. a factor of 10 higher than the normal ionization cross section shown on Figure 10. However, since this resonance line is rather narrow (10^{-1} Å), the solar spectrum needs to be known with sufficient resolution before introducing the high absorption cross section in a computation of the ionization coefficient.

Below 190 Å, photoionization of helium leads to He^+ with $n=2$ or $n=1$. Samson (1969) showed that about 8% the ions formed at 186 Å are excited in the $n=2$ state. These excited ions can emit the important 304 Å line, and according to Samson (1969), helium could act as a continuous absorber of radiation with $\lambda < 189$ Å and reemit this integrated energy into the 304 Å line. Figure 11 shows the ionization cross section in the soft X-ray region. Above 50 Å the agreement between the values of Lowry *et al.* (1965) and those of Denne (1970) is satisfactory. For $\lambda < 50$ Å, the two experimental values obtained by Denne (1970) disagree with the semiempirical values deduced by Victoreen (1949) and by Henke *et al.* (1957). It is to be noted that this wave-

length region provides, however, a negligible contribution to the normal ionization coefficient.

The major uncertainty in the photoionization rate results from an incomplete knowledge of the solar spectrum below 500 Å. Besides the difficulties associated with the absolute calibration of the UV spectrometers, the variation with solar activity is not yet quantitatively known. The most widely values used in aeronomic calculations are those recommended by Hinteregger (1970) for medium solar activity and non-flaring conditions. With these values for the solar flux and the ionization cross-sections from Figures 10 and 11, one obtains the helium ionization coefficients given in Table VI for different solar lines and wavelength intervals. The total photoionization

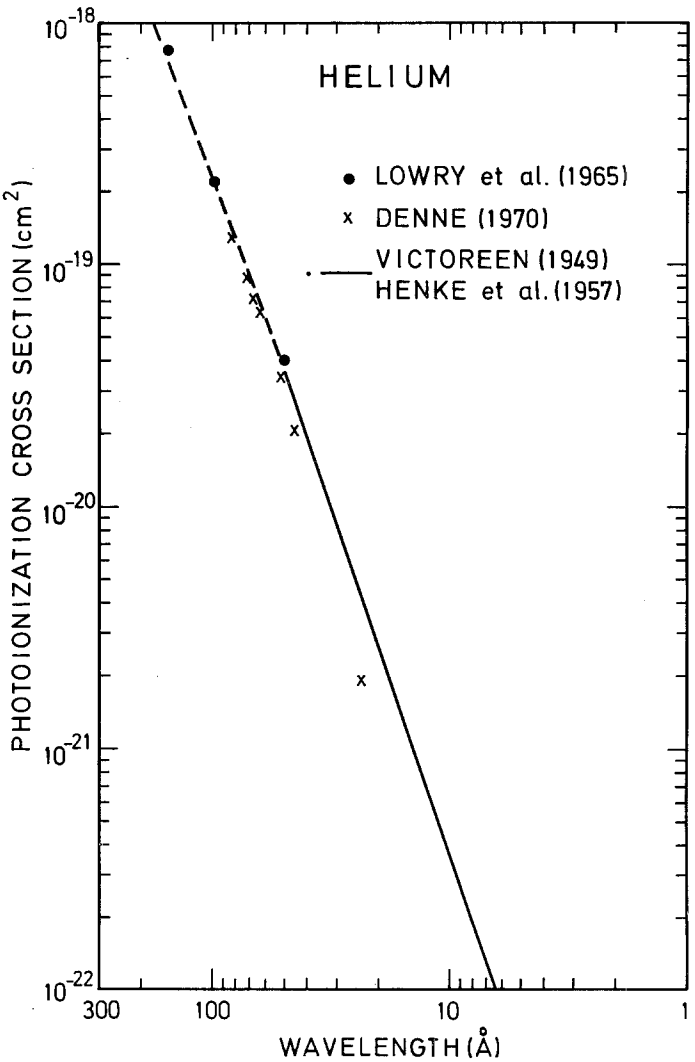

Fig. 11. Helium-4 photoionization cross section by soft X-rays.

TABLE VI

He^4 ionization coefficient with the solar fluxes of Hinteregger (1970)

Wavelength (Å)	Flux (10^9 ph cm^{-2} s^{-1})	σ(He) (10^{-18} cm^2)	I_∞(He) (s^{-1})
504	0.50	7.4	3.7×10^{-9}
499.3	0.38	7.3	2.8×10^{-9}
465.2	0.16	6.5	1.0×10^{-9}
630–460	0.44	6.8	3.0×10^{-9}
460–370	0.63	5.1	3.2×10^{-9}
368.1	0.56	4.3	2.4×10^{-9}
364.8	0.17	4.2	7.1×10^{-10}
360.7	0.36	4.1	1.5×10^{-9}
335.4	0.72	3.5	2.5×10^{-9}
303.8	5.4	2.8	1.5×10^{-8}
284.1	1.1	2.4	2.6×10^{-9}
370–280	2.03	3.4	6.9×10^{-9}
280–231	3.1	2.0	6.2×10^{-9}
231–205	1.4	1.4	2.0×10^{-9}
205–176	3.7	1.2	4.4×10^{-9}
176–153	0.9	0.83	7.5×10^{-10}
153–100	0.4	0.44	1.8×10^{-10}
100–90	0.099	0.20	2.0×10^{-11}
90–80	0.12	0.16	1.9×10^{-11}

coefficient is 6×10^{-8} s^{-1} and the effect of the wavelength region below 100 Å is almost negligible. Presently available experimental data cannot lead to a detailed picture of the solar cycle variation. The HeII line at 304 Å analyzed by Timothy and Timothy (1970) is characterized by an average flux of 8.8×10^9 photons cm^{-2} s^{-1} with a long term variation of 20% and a short term flare increase of 25%. Solar flare observations on OSO 4 in 1967 indicate however enhancements between 1.8 and 3.8 (Wood *et al.*, 1972). Nevertheless, the entire solar UV spectrum does not necessarily follow the behavior of a particular emission line.

In order to have an idea of the solar cycle variation, Table VII gives solar UV fluxes over larger wavelength intervals, which have been used by Banks and Kockarts (1973) for aeronomic computations. The errors quoted in Table VII are intended to reflect real solar cycle variations as well as possible systematic errors in the experimental data. The cross sections are rough average values deduced from Figure 10.

TABLE VII

Helium-4 ionization coefficient

Wavelength (Å)	Flux (10^9 ph cm^{-2} s^{-1})	σ(He) (cm^2)	I_∞(He) (s^{-1})
504–375	4 ± 2	6×10^{-18}	$(2.4 \pm 1.2) \times 10^{-8}$
375–275	14 ± 6	3×10^{-18}	$(4.1 \pm 1.9) \times 10^{-8}$
275–150	14 ± 6	1×10^{-18}	$(1.4 \pm 0.6) \times 10^{-8}$
150–80	1.3 ± 0.7	3×10^{-19}	$(3.8 \pm 2.2) \times 10^{-10}$

From Table VII, it is seen that the total photoionization coefficient is given at the top of the atmosphere by

$$I_\infty(\mathrm{He}) = (8 \pm 4) \times 10^{-8}\ \mathrm{s}^{-1}. \tag{27}$$

A variation of a factor of 3 is therefore possible between quiet and disturbed solar conditions. This example stresses again the necessity for continuous measurements of the whole solar UV spectrum since such a variation for the ionization coefficient cannot be ignored in ionospheric studies.

Another source of He^+ ions results from electron impact ionization. Cross sections have been measured by several authors (see Rapp and Englander-Golden, 1965; Schram *et al.*, 1965; Schram *et al.*, 1966). Recently cross sections for production of secondary electrons in the energy range from 0 to 1 eV have also been measured (Grissom *et al.*, 1972). Analytical expressions for the total ionization cross sections are also available (Green and Sawada, 1972). The cross sections (curves and points) in Figure 6 and the curves in Figures 5 and 7 of Green and Sawada (1972) as well as the values of K_σ in their Table II should be multiplied by 0.7739 due to an error in the normalization factors. The correct values are given by the full curve on the present Figure 12. The analytic expression for the ionization cross section $\sigma(E)$ in cm^2 as a function of the electron energy E in eV can be written for the range 25 eV $\leqslant$ $\leqslant E \leqslant 3000$ eV

$$\sigma(E) = 2.015 \times 10^{-15} \ln(E/1.32) \times [\mathrm{arctg}\, A + \mathrm{arctg}\, B]/(E + 24.5) \tag{28}$$

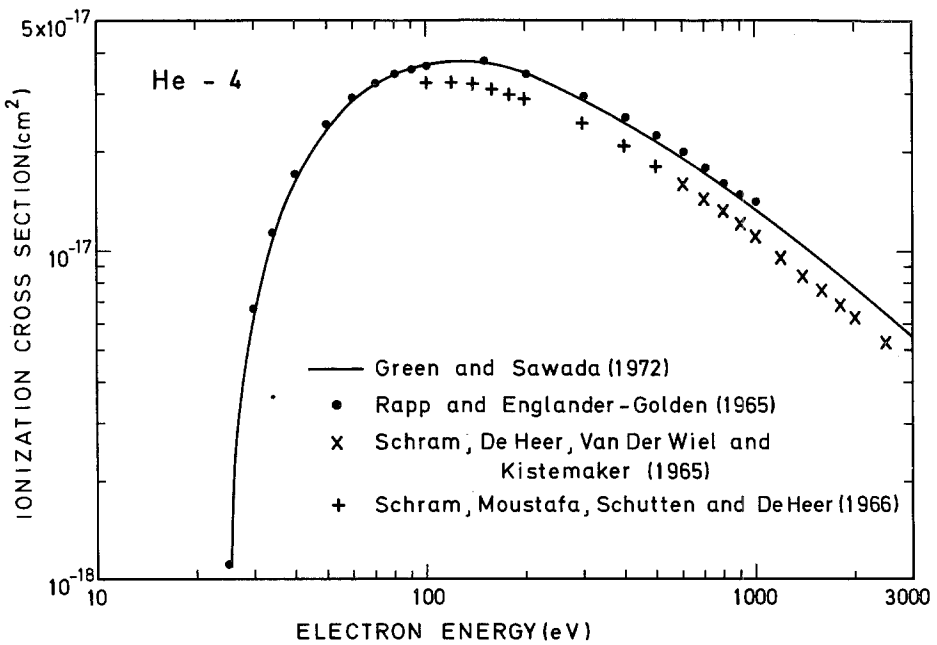

Fig. 12. Electron impact ionization cross section for helium-4.

with

$$A = (0.5\,E^3 + 26.75\,E^2 + 865.25\,E + 12495)/(15.5\,E^2 + 759.5\,E) \quad (29)$$

and

$$B = -\,(2.25\,E^2 + 1165.4\,E + 27201)/(15.5\,E^2 + 759.5\,E). \quad (30)$$

Figure 12 shows that a flux of the order of 3×10^8 electrons $cm^{-2}\,s^{-1}$ at 100 eV is required to give an ionization coefficient of the order of $10^{-8}\,s^{-1}$ indicating that electron impact ionization is normally negligible.

The chemical loss processes of He^+ ions in the ionosphere can be written as

$$\gamma_1;\ He^+(^2S) + O_2(X^3\Sigma_g^-) \rightarrow He(^1S) + O(^3P) + O^+(^4S) + 5.85\ eV \quad (31)$$

$$\gamma_1^*;\ He^+(^2S) + O_2(X^3\Sigma_g^-) \rightarrow He(^1S) + O_2^+(X^2\Pi_g) + 12.25\ eV \quad (32)$$

$$\gamma_2;\ He^+(^2S) + N_2(X^1\Sigma_g^+) \rightarrow He(^1S) + N(^4S) + N^+(^3P) + 0.28\ eV \quad (33)$$

$$\gamma_2^*;\ He^+(^2S) + N_2(X^1\Sigma_g^+) \rightarrow He(^1S) + N_2^+(C^2\Sigma_u)_{v=3,4} \quad (34)$$

$$\gamma_3;\ He^+(^2S) + NO(X^2\Pi) \rightarrow He(^1S) + O(^3P) + N^+(^3P) + 3.54\ eV, \quad (35)$$

where the reaction rate coefficients γ are not less than $10^{-9}\,cm^3\,s^{-1}$. For the reactions with molecular oxygen, Warneck (1967) measured the rate coefficient $\gamma_1 = 1.2\times10^{-9}$ $cm^3\,s^{-1}$ and $\gamma_1^* < 2\times10^{-10}\,cm^3\,s^{-1}$. The reactions with molecular nitrogen have been discussed by Ferguson (1969) who gives a rate coefficient $\gamma_2+\gamma_2^* = (1.4\pm0.3)\times10^{-9}$ $cm^3\,s^{-1}$. The rate coefficient for the reaction with NO is $\gamma_3 = 1.5\times10^{-9}\,cm^3\,s^{-1}$ (Fehsenfeld *et al.*, 1966) or $\gamma_3 = 2.0\times10^{-9}\,cm^3\,s^{-1}$ (Moran and Friedman, 1966). Reaction (34) was thought to involve the $N_2^+(^2\Sigma_g^+)$ ground state. In this case an excess kinetic energy of 9.01 eV could be shared between He and N_2^+ in a way such that He atoms could escape from the gravitational field. Patterson (1968) showed that this mechanism is probably not effective for an appropriate helium balance since the excess energy is actually placed in internal energy of N_2^+ (Ferguson, 1969; Koopman, 1969) which can than lead to radiation or to a predissociation process into N and N^+.

Above the F_2 peak, the reactions with N_2 are the most important loss processes for He^+ and the time constant associated with the He^+ loss is roughly (see Banks and Kockarts, 1973)

$$\tau(He^+) \sim 10^9/[n(O_2) + n(N_2)]. \quad (36)$$

At 300 km $\tau(He^+)$ ranges from 2 to 30 s when the thermosphere temperature varies from 2000 K to 750 K. Since the corresponding time constant for H^+ is somewhat smaller, transport processes are more important for He^+ than for H^+. Above 500 to 700 km the ion distribution is controlled by electric and magnetic fields, gravity and ion partial pressure gradients. A detailed description of plasma motions and the coupling between the topside ionosphere and the magnetosphere is given by Banks and Kockarts (1973).

6. Helium Balance

The problem of the helium balance was clearly stated, more than fifteen years ago, by Nicolet (1957) and by Bates and McDowell (1957). It was found that He^4 atoms could not escape from the atmosphere as rapidly as they are released from the Earth unless the temperature at the base of exosphere is very high.

The total column contents of He^4 and He^3 at ground level are respectively $1.13 \times \times 10^{20}$ cm^{-2} and 1.41×10^{14} cm^{-2}. With a He^4 production flux of $(2.5 \pm 1.5) \times 10^6$ cm^{-2} s^{-1}, the present atmospheric content can be supplied in approximately $(2.3 \pm 1.3) \times 10^6$ yr. This implies that atmospheric helium-4 has been renewed approximately 1000 to 2000 times since the Earth's formation. With a He^3 production flux of the order of (7.5 ± 2.5) cm^{-2} s^{-1}, a similar calculation leads to a production time of only $(6.7 \pm 2.2) \times 10^5$ yr. Without an effective escape mechanism, a constant helium-4 influx of 2.5×10^6 cm^{-2} s^{-1} would have lead to a column content of 3.5×10^{23} cm^{-2} since the Earth's formation. In this hypothetical case, the present mixing ratio of He^4 at ground level would be 1.6×10^{-3}. Such a high value is completely unacceptable and an effective escape mechanism *must* therefore exist in order to avoid a continuous accumulation of helium-4 over geological time. The different attempts to explain the atmospheric helium balance are based either on kinetic escape of the neutral atoms or on an ionic escape along the open lines of the Earth's geomagnetic field.

The neutral escape process occurs over the whole Earth above some critical level where collisions can be neglected. For a Maxwellian velocity distribution function, the escape flux is controlled by an effusion velocity (see Nicolet, 1957)

$$v_1 = (g/2\pi)^{1/2} \, r H_1^{1/2} \, (1 + H_1/r) \, e^{-r/H_1}, \tag{37}$$

where r is the geocentric distance of the critical level and $H_1 = kT/m_1 g$ is the scale height of the escaping constituent. The effusion velocity varies strongly with the temperature T and with the mass m_1 of the light constituent. Since the height variation of the escape flux $n_1 v_1$ is small, it is possible to adopt a critical level independent of the thermopause temperature.

Kockarts and Nicolet (1962) deduced a helium-4 thermal escape flux of 6×10^4 cm^{-2} s^{-1} for the period 1951–1961. This flux is insufficient to assure a balance with the production from within the Earth. The He^3 thermal escape flux for the same period was 3.5 cm^{-2} s^{-1}, i.e. a value comparable with the production flux. For the period 1947–1968, Johnson and Axford (1969) deduced a He^3 thermal escape flux of 5.9 cm^{-2} s^{-1}. The difference between these estimations results essentially from the very high solar activity maximum in 1947. In both computations the daily thermopause temperature was obtained from an empirical relation between the temperature and the solar decimetric radioelectric flux. The correction due to geomagnetic activity was omitted as well as the possibility of greatly elevated thermospheric temperatures over the polar caps during magnetic storms. The nighttime minimum thermopause temperature $T_{\min}$ is given by (Jacchia, 1971)

$$T_{\min} = 379 + 3.24 \, \bar{S}_{10.7} + 1.3 \, (S_{10.7} - \bar{S}_{10.7}), \tag{38}$$

where $S_{10.7}$ is the daily solar radiolectric flux at 10.7 cm measured in 10^{-22} watt m^{-2} Hz^{-1} and $\bar{S}_{10.7}$ is the mean value over three solar rotations. The daytime maximum temperature is simply $1.3 \times T_{min}$. The temperature increase ΔT resulting from geomagnetic activity is expressed by (Jacchia *et al.*, 1967)

$$\Delta T = 28 K_p + 0.03 \exp(K_p), \tag{39}$$

where K_p is considered here as the daily mean value of the three hours geomagnetic planetary index. A daily computation with expressions (37) to (39) leads to the average effusion velocities given in Table VIII for the period 1958, February 8 through 1971,

TABLE VIII

Average effusion velocities (cm s^{-1}) for the period 8 February, 1958 through 4 May, 1971

Altitude 500 km	Without geomagnetic effect		With geomagnetic effect	
	Night	Day	Night	Day
He^4	5.1×10^{-6}	1.1×10^{-3}	2.8×10^{-5}	3.0×10^{-3}
He^3	1.8×10^{-3}	1.1×10^{-1}	5.9×10^{-3}	2.2×10^{-1}

May 4. Table VIII indicates large variations of the effusion velocities and it is clear that the geomagnetic effect cannot be neglected especially for nighttime conditions since the relative increase $\Delta T/T$ is greater than during the day. The rather small values of Table VIII are a direct consequence of the weak solar activity maximum in 1968–1969. When a similar computation is made from 1957, July 7, through 1971, May 4, the average effusion velocity is 2.7×10^{-3} cm s^{-1} for He^4 and 2.0×10^{-1} cm s^{-1} for He^3 without the effect of geomagnetic activity. It is therefore insufficient to determine an average effusion velocity or an average escape flux for only a few solar cycles when the helium balance is determined over a time scale of several million years.

A few years ago, a controversy arose about the accuracy of the effusion velocity given by expression (37) since the escape flux causes a distortion of the assumed Maxwellian velocity distribution function. This problem is usually investigated with a Monte Carlo technique. Recently, Chamberlain and Smith (1971) and Brinkmann (1971) reanalyzed the question and it appears now that the effusion velocity (37) is a sufficiently good approximation for the case of helium.

A greater difficulty results from the presence of the winter helium bulge since the concentration variations at the critical level are much larger than the changes induced by temperature variations. Figures 13 and 14 indicate how He^3 and He^4 can vary at 500 km height. Even if variations of the eddy diffusion coefficient around 100 km are not the explanation of these changes, observations of the helium bulge (Reber *et al.*, 1971) show that the helium concentration can increase by a factor of ten from summer to winter hemisphere. A detailed computation of the thermal escape requires, therefore, a complete knowledge of the He^4 and He^3 distributions over the entire

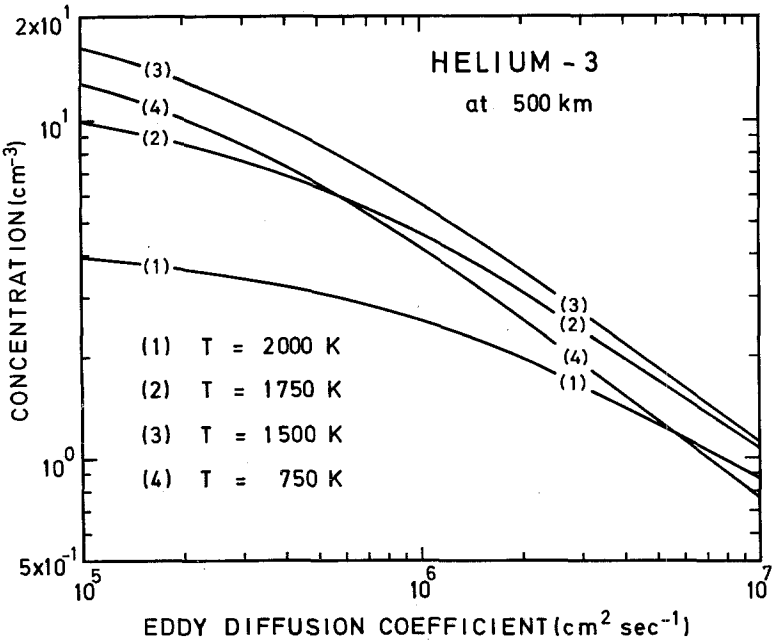

Fig. 13. Helium-3 concentration at 500 km as a function of eddy diffusion coefficient for thermopause temperatures of 2000, 1750, 1500 and 750K.

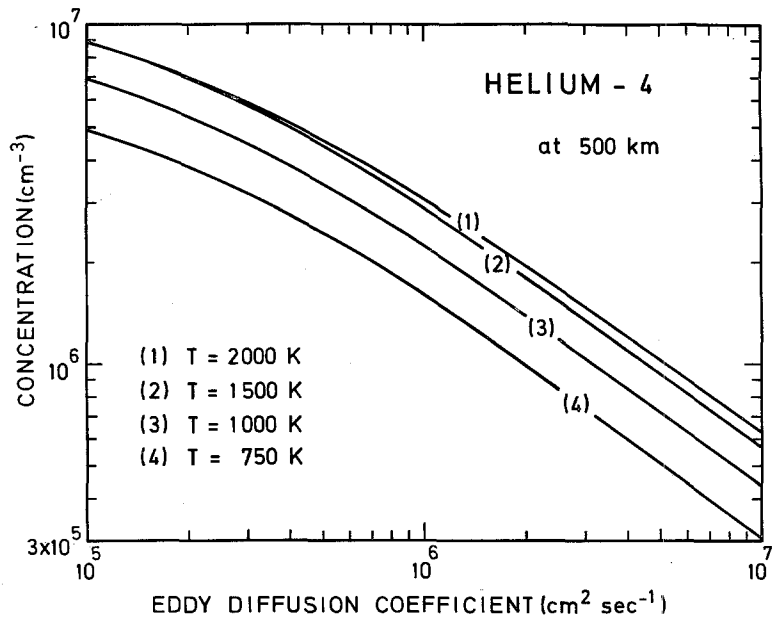

Fig. 14. Helium-4 concentration at 500km as a function of eddy diffusion coefficient for thermopause temperatures of 2000, 1500, 1000 and 750K.

TABLE IX

Possible escape fluxes ($cm^{-2}\ s^{-1}$) at 500 km

Helium-4 $K(cm^2\ s^{-1})$	Thermopause temperature (K)					
	750	1000	1250	1500	1750	2000
0	1.0×10^{-3}	1.3×10^{1}	3.7×10^{3}	7.8×10^{5}	2.1×10^{6}	1.3×10^{7}
1×10^{5}	7.1×10^{-4}	9.4×10^{0}	2.6×10^{3}	5.7×10^{5}	1.5×10^{6}	9.6×10^{6}
1×10^{6}	2.3×10^{-4}	3.1×10^{0}	8.7×10^{2}	1.9×10^{5}	4.9×10^{5}	3.4×10^{6}
6×10^{6}	6.5×10^{-5}	8.7×10^{-1}	2.5×10^{2}	5.5×10^{4}	1.4×10^{5}	9.9×10^{5}
1×10^{7}	4.5×10^{-5}	6.0×10^{-1}	1.7×10^{2}	3.8×10^{4}	9.9×10^{4}	7.0×10^{5}
Helium-3						
0	2.1×10^{-5}	2.5×10^{-2}	1.6×10^{0}	2.2×10^{1}	8.6×10^{1}	1.3×10^{2}
1×10^{5}	1.5×10^{-5}	1.8×10^{-2}	1.2×10^{0}	1.7×10^{1}	7.1×10^{1}	1.2×10^{2}
1×10^{6}	5.1×10^{-6}	6.0×10^{-3}	4.0×10^{-1}	5.9×10^{0}	3.3×10^{1}	7.8×10^{1}
6×10^{6}	1.4×10^{-6}	1.6×10^{-3}	1.1×10^{-1}	1.7×10^{0}	1.1×10^{1}	3.5×10^{1}
1×10^{7}	9.3×10^{-7}	1.0×10^{-3}	7.5×10^{-2}	1.2×10^{0}	7.8×10^{0}	2.6×10^{1}

globe. Table IX shows how the escape flux varies simultaneously with the temperature and with the eddy diffusion coefficient, i.e. with latitude. It can been seen that the fluxes of Table IX are still smaller than the maximum diffusion fluxes discussed in Section 4. Furthermore the temperature must still be higher than 1250 K in order for there to be an approach to the balance between production and loss. The temperature variation of the He^3 escape flux is less important since for high temperatures the helium-3 behavior is similar to deuterium (Kockarts, 1972b). It is clear that thermal escape cannot lead to a permanent equilibrium between production and loss. During certain periods, such as high solar activity or geomagnetic disturbances, thermal escape is however an important factor for the helium balance.

Ionic processes such as (34) have been suggested as a channel which produces neutral atoms with enough kinetic energy to escape from the Earth's gravitational field. In a discussion of non-thermal processes, Patterson (1968) showed that these mechanisms are not effective.

The best candidate for an adequate helium balance is the polar wind (Axford, 1968; Banks and Holzer, 1968) which provides a loss mechanism for the He^+ ions produced by photoionization at a rate almost identical to the neutral helium influx from the Earth's surface. According to Banks and Holzer (1969) the polar wind can lead to an escape of 2 to 4×10^6 ions $cm^{-2}\ s^{-1}$ resulting from the photoionization of He^4. A kinetic theory of the polar wind (Lemaire and Scherer, 1970; Lemaire, 1972) can be used to compute the He^+ bulk velocity as a function of the ion temperature. Figure 15 gives an example of such a computation made by J. Lemaire. With a bulk velocity of the order of 1 km s^{-1} at 1000 km height, a helium ion concentration of 20 to 40 cm^{-3} is required, for a flux comparable to the values obtained by Banks and Holzer (1969). The helium-3 non-thermal escape flux is estimated of the order of 1.25 $cm^{-2}\ s^{-1}$ by Johnson and Axford (1969) when the He^+ flux is 10^6 $cm^{-2}\ s^{-1}$. This value leads to a total He^3 escape flux of approximately 7.5 $cm^{-2}\ s^{-1}$, i.e. a value

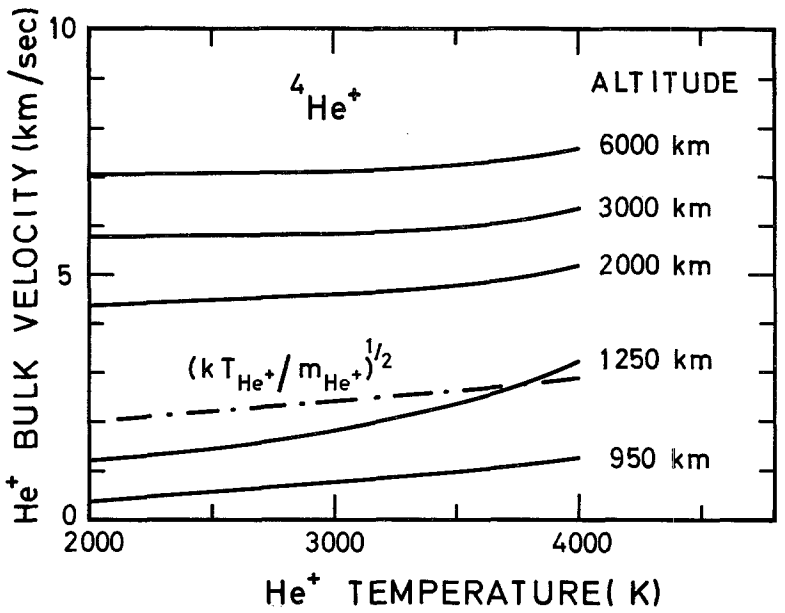

Fig. 15. Velocities of He^+ ions at different heights as a function of the ionic temperature. The dotted-dashed curve indicates the transition from subsonic to supersonic flow. (J. Lemaire, personal communication).

compatible with the production flux discussed in Section 3. It is however difficult to analyze in detail the polar wind effect on the helium balance, since the boundary between convection and co-rotation of magnetic field lines is somewhat variable.

Another possibility has been proposed by Sheldon and Kern (1972), who suggest that the loss of He^4 is caused by the direct interaction of the solar wind with the upper atmosphere for only short periods of time during reversals of the geomagnetic field. During these periods the He^3 abundance is enhanced by cosmic-ray spallation during the low dipole field periods subsequent to the reversals. A non equilibrium helium atmosphere is obtained and the concentrations fluctuate over geological time scale. During a 300 yr period of zero field (if this is possible), about 5% of the present helium atoms could be removed by an average ion loss rate of 10^9 cm^{-2} s^{-1}. Sheldon and Kern (1972) conclude that 20 geomagnetic field reversals are enough over the last 3.5×10^6 yr period to assure a balance between production and loss. Such a discontinuous removal requires however a replacement from below. Sheldon and Kern (1972) deduce that molecular diffusion can supply a flux of 4×10^9 cm^{-2} s^{-1} at 110 km. Such a value is however at least a factor of 10 higher than the maximum diffusion flux obtained in Section 4. Therefore one should also consider that helium could be quickly exhausted in the upper atmosphere during a geomagnetic field reversal. The supply from below is than to small for an adequate helium balance. Further investigations are therefore necessary to determine wether or not the mechanism proposed by Sheldon and Kern (1972) is really effective.

It is clear that the helium balance problem is not yet completely solved since detailed calculations including simultaneously thermal escape and polar wind escape have not yet been performed.

7. Conclusion

Production, distribution and escape are the three keys needed to understand the terrestrial helium problem. This implies that measurements are required from the deep sea up to the edge of interplanetary space. A uniform explanation of the physical situation involves therefore several different techniques including sea and air sampling, mass spectrometric detection of ions and neutrals by rockets and satellites as well optical observations in the infrared and in the extreme ultraviolet.

The solution of the He^4 production problem requires more measurements in the deep sea at different geographical locations. In such a way a global map could possibly be established for the He^4 outgassing. In addition to the implications for atmospheric helium, it is clear that important oceanographic results would come out of such a project. Furthermore, the geochemical distribution of the radioactive isotopes is not known with enough accuracy to determine unambigously the He^4 production in the Earth. The interpretation of the deep sea measurements is however still subject to some uncertainty with regard to the origin of the observed He^4 excess. With the present knowledge of the Earth's composition the He^4 outflow is $(2.5 \pm 1.5) \times 10^6$ $cm^{-2}\,s^{-1}$. The He^3 production is still subject to large uncertainties. A flow of (7.5 ± 2.5) $cm^{-2}\,s^{-1}$ is due mainly to auroral precipitation and to a flux observed in the deep sea. It would be very interesting to have He^3 measurements in the homosphere below 100 km and in the lower exosphere since the local deposition of this isotope could then be determined. Furthermore, a simultaneous production of He^3 at high and low altitudes probably affects the vertical distribution.

Mass spectrometric measurements in the thermosphere and lower exosphere now give some indications on the possible transport mechanisms for helium. Since it is very difficult to perform measurements in the 90 to 120 km region, it is useful to interpret measurements around 500 km altitudes in terms of phenomena occuring at much lower altitudes. Satellite and rocket data obtained well above the turbopause are therefore a good tool to investigate the transition region from mixing to diffusion transport. The observed concentration variation of a factor of 10 between summer and winter hemisphere around 500 km should be continously monitored in order to obtain a global picture of the helium bulge as a function of time. Such an analysis would allow a detailed computation of the thermal escape. Magnetospheric observations of the convection zone are also required for long term estimations of the polar wind effect on the helium balance. Ultraviolet observations of the 504 and 304 Å line will also provide fundamental informations on the helium distribution along particular line of sight. The 304 Å line, in particular, seems to offer a promissing technique for the mapping of magnetosphere movements.

The presence of helium from ground level up to the interplanetary medium offers

a powerful possibility to use this inert constituent as a tracer representing complex physical phenomena.

Acknowledgements

The author expresses his thanks to Dr M. Nicolet who suggested this topic and to Drs P. M. Banks and J. Lemaire for their valuable comments.

References

Aldrich, L. T. and Nier, A. O.: 1948, *Phys. Rev.* **74**, 1590.
Axford, W. I.: 1968, *J. Geophys. Res.* **73**, 6855.
Axford, W. I.: 1970, in B. M. McCormac (ed.), *Particles and Fields in the Magnetosphere*, D. Reidel, Dordrecht-Holland, pp. 46–59.
Banks, P. M.: 1972, in E. R. Dyer (ed.), *Critical Problems of Magnetospheric Physics*, IUCSTP, Washington DC, pp. 157–178.
Banks, P. M. and Holzer, T. E.: 1968, *J. Geophys. Res.* **73**, 6846.
Banks, P. M. and Holzer, T. E.: 1969, *J. Geophys. Res.* **74**, 6317.
Banks, P. M. and Kockarts, G.: 1973, *Aeronomy*, Part A and B, Academic Press, New York.
Bates, D. R. and McDowell, M. C. R.: 1957, *J. Atmospheric Terrest. Phys.* **11**, 200.
Bates, D. R. and Patterson, T. N. L.: 1962, *Planetary Space Sci.* **9**, 599.
Bauer, S. J.: 1966, *Ann. Geophys.* **22**, 247.
Bieri, R. H.: 1971, *Earth Planetary Sci. Letters* **10**, 329.
Bieri, R. H. and Koide, M.: 1972, *J. Geophys. Res.* **77**, 1667.
Bieri, R. H., Koide, M., and Goldberg, E. D.: 1964, *Science* **146**, 1035.
Bieri, R. H., Koide, M., and Goldberg, E. D.: 1966, *J. Geophys. Res.* **71**, 5243.
Bieri, R. H., Koide, M., and Goldberg, E. D.: 1967, *J. Geophys. Res.* **72**, 2497.
Bieri, R. H., Koide, M., Martell, E. A., and Scholz, T. G.: 1970, *J. Geophys. Res.* **75**, 6731.
Bitterberg, W., Bruchhausen, K., Offermann, D., and von Zahn, U.: 1970, *J. Geophys. Res.* **75**, 5528.
Blamont, J.-E. and Baguette, J. M.: 1961, *Ann. Geophys.* **17**, 319.
Blamont, J.-E. and De Jager, C.: 1961, *Ann. Geophys.* **17**, 134.
Bourdeau, R. E., Whipple, E. C., Jr., Donley, J. L., and Bauer, S. J.: 1962, *J. Geophys. Res.* **67**, 167.
Brandt, J. C., Broadfoot, A. L., and McElroy, M. B.: 1965, *Astrophys. J.* **141**, 1584.
Brinkmann, R. T.: 1971, *Planetary Space Sci.* **19**, 791.
Cairns, R. B. and Samson, J. A. R.: 1965, *J. Geophys. Res.* **70**, 99.
Cameron, A. G. W.: 1968, in L. H. Ahrens (ed.), *Origin and Distribution of the Elements*, Pergamon Press, London, pp. 125–143.
Carlson, R. W.: 1972, *J. Geophys. Res.* **77**, 6282.
Chamberlain, J. W. and Smith, G. R.: 1971, *Planetary Space Sci.* **19**, 675.
Chapman, S. and Cowling, T. G.: 1960, *The Mathematical Theory of Non-Uniform Gases*, 2nd ed., Cambridge at the University Press, p. 244.
Chapman, S. and Milne, E. A.: 1920, *Quart. J. Roy. Meteorol. Soc.* **46**, 357.
Christensen, A. B., Patterson, T. N. L., and Tinsley, B. A.: 1971, *J. Geophys. Res.* **76**, 1764.
Clarke, W. B., Beg, M. A., and Craig, H.: 1969, *Earth Planetary Sci. Letters* **6**, 213.
Clarke, W. B., Beg, M. A., and Craig, H.: 1970, *J. Geophys. Res.* **75**, 7676.
Colegrove, F. D., Hanson, W. B., and Johnson, F. S.: 1965, *J. Geophys. Res.* **70**, 4931.
Cook, G. E.: 1967, *Planetary Space Sci.* **15**, 627.
Coon, J. H.: 1949, *Phys. Rev.* **75**, 1355.
Craig, H. and Clarke, W. B.: 1970, *Earth Planetary Sci. Letters* **9**, 45.
Craig, H. and Weiss, R. F.: 1971, *Earth Planetary Sci. Letters* **10**, 289.
Denne, D. R.: 1970, *J. Phys. D, Appl. Phys.* **3**, 1392.
Donahue, T. M.: 1969, *J. Geophys. Res.* **74**, 1128.
Fairhall, A. W.: 1969, *Earth Planetary Sci. Letters* **7**, 249.
Fehsenfeld, F. C., Schmeltekopf, A. L., Goldan, P. D., Schiff, H. I., and Ferguson, E. E.: 1966, *J. Chem. Phys.* **44**, 4087.

Frankland, E. and Lockyer, J. N.: 1869, *Proc. Roy. Soc., London* **17**, 288.
Glückauf, E.: 1946, *Proc. Roy. Soc.* **A185**, 98.
Glückauf, E. and Paneth, F. A.: 1946, *Proc. Roy. Soc.* **A185**, 89.
Goldberg, L.: 1962, *Astrophys. J.* **136**, 1154.
Green, A. E. S. and Sawada, T.: 1972, *J. Atmospheric Terrest. Phys.* **34**, 1719.
Grissom, J. T., Compton, R. N., and Garrett, W. R.: 1972, *Phys. Rev. A* **6**, 977.
Hanson, W. B.: 1962, *J. Geophys. Res.* **67**, 183.
Henke, B. L., White, R., and Lundberg, B.: 1957, *J. Appl. Phys.* **28**, 98.
Heydemann, A.: 1969, in K. H. Wedepohl (ed.), *Handbook of Geochemistry*, vol. I, Springer-Verlag, Berlin, pp. 376–412.
Heymann, D.: 1971, in B. Mason (ed.), *Handbook of Elemental Abundances in Meteorites*, Gordon and Breach, New York, pp. 29–66.
Hickman, D. R. and Nier, A. O.: 1972, *J. Geophys. Res.* **77**, 2880.
Hinteregger, H. E.: 1970, *Ann. Geophys.* **26**, 547.
Hodges, R. R., Jr.: 1970, *J. Geophys. Res.* **75**, 4842.
Jacchia, L. G.: 1971, *Smiths. Astrophys. Obs. Spec. Rep.* **332**, 111 pp.
Jacchia, L. G., Slowey, J., and Verniani, F.: 1967, *J. Geophys. Res.* **72**, 1423.
Janssen, J.: 1868, *Compt. Rend. Acad. Sci. Paris* **67**, 838.
Jeans, J. H.: 1925, *The Dynamical Theory of Gases*, Dover, New York, p. 340.
Jenkins, W. J., Beg, M. A., Clarke, W. B., Wangersky, P. J., and Craig, H.: 1972, *Earth Platetary Sci. Letters* **16**, 122.
Johnson, H. E. and Axford, W. I.: 1969, *J. Geophys. Res.* **74**, 2433.
Johnson, F. S. and Gottlieb, B.: 1970, *Planetary Space Sci.* **18**, 1707.
Kasprzak, W. T.: 1969, *J. Geophys. Res.* **74**, 894.
Kasprzak, W. T., Krankowsky, D., and Nier, A. O.: 1968, *J. Geophys. Res.* **73**, 6765.
Kayser, H.: 1895, *Chem. Z.* **19**, 1549.
Keating, G. M. and Prior, E. J.: 1968, *Space Res.* **8**, 982.
Keating, G. M., Mullins, J. A., and Prior, E. J.: 1970, *Space Res.* **10**, 439.
Keating, G. M., Prior, E. J., Levine, J. S., and Mullins, J. A.: 1972, *Space Res.* **12**, 763.
Keneshea, T. J. and Zimmerman, S. P.: 1970, *J. Atmospheric Sci.* **27**, 831.
Kockarts, G.: 1963, *Bull. Acad. Roy. Belgique, Cl. Sci.* **49**, 1135.
Kockarts, G.: 1971, in F. Verniani (ed.), *Physics of the Upper Atmosphere*, Editrice Compositori, Bologna, Italy, pp. 330–347.
Kockarts, G.: 1972a, *J. Atmospheric Terrest. Phys.* **34**, 1729.
Kockarts, G.: 1972b, *Space Res.* **12**, 1047.
Kockarts, G. and Nicolet, M.: 1962, *Ann. Geophys.* **18**, 269.
Kockarts, G. and Nicolet, M.: 1963, *Ann. Geophys.* **19**, 370.
Koopman, D. W.: 1969, *Phys. Rev.* **178**, 161.
Krankowsky, D., Kasprzak, W. T., and Nier, A. O.: 1968, *J. Geophys. Res.* **73**, 7291.
Larimer, J. W.: 1971, *Geochim. Cosmochim. Acta* **35**, 769.
Lemaire, J.: 1972, *J. Atmospheric Terrest. Phys.* **34**, 1647.
Lemaire, J. and Scherer, M.: 1970, *Planetary Space Sci.* **18**, 103.
Lettau, H.: 1951, in T. F. Malone (ed.), *Compendium of Meteorology*, American Meteorological Society, Boston, pp. 320–332.
Lloyd, K. H., Low, C. H., McAvaney, B. J., Rees, D., and Roper, R. G.: 1972, *Planetary Space Sci.* **20**, 761.
Lowry, J. F., Tomboulian, D. H., and Ederer, D. L.: 1965, *Phys. Rev.* **137**, A1054.
MacDonald, G. J. F.: 1963, *Rev. Geophys.* **1**, 305.
MacDonald, G. J. F.: 1964, *J. Geophys. Res.* **69**, 2933.
Madden, R. P. and Codling, K.: 1965, *Astrophys. J.* **141**, 364.
Mange, P.: 1955, *Ann. Geophys.* **11**, 153.
Mange, P.: 1960, *J. Geophys. Res.* **65**, 3833.
Mange, P.: 1961, *Ann. Geophys.* **17**, 277.
Mange, P.: 1973, in B. M. McCormac (ed.), *Physics and Chemistry of Upper Atmospheres*, Reidel, Dordrecht-Holland, 248–259.
Meadows, E. B. and Towsend, J. W.: 1958, *Ann. Geophys.* **14**, 80.
Meier, R. R. and Weller, C. S.: 1972, *J. Geophys. Res.* **77**, 1190.

Moran, T. F. and Friedman, L.: 1966, *J. Chem. Phys.* **45**, 3837.
Morgan, J. W. and Lovering, J. F.: 1967, *Nature, London* **213**, 873.
Müller, D. and Hartmann, G.: 1969, *J. Geophys. Res.* **74**, 1287.
Namba, O.: 1965, *Astrophys. J.* **141**, 827.
Nicolet, M.: 1957, *Ann. Geophys.* **13**, 1.
Nicolet, M.: 1961, *J. Geophys. Res.* **66**, 2263.
Nicolet, M.: 1968, *Geophys. J. Roy. Astron. Soc.* **15**, 157.
Ozima, M. and Kudo, K.: 1972, *Nature Phys. Sci., London* **239**, 23.
Patterson, T. N. L.: 1968, *Rev. Geophys.* **6**, 553.
Pokhunkov, A. A.: 1962, *Iskusst. Sputniki Zemli, Akad. Nauk SSSR* **13**, 110.
Ramsay, W.: 1895, *Proc. Roy. Soc. London* **58**, 65.
Ramsay, W.: 1905, *Proc. Roy. Soc. London* **76A**, 111.
Ramsay, W.: 1908, *Proc. Roy. Soc. London* **80A**, 599.
Rayet, G.: 1869, *Compt. Rend. Acad. Sci. Paris* **68**, 320.
Rapp, D. and Englander-Golden, P.: 1965, *J. Chem. Phys.* **43**, 1464.
Reber, C. A.: 1971, *Goddard Space Flight Center X-621-71-480*, Greenbelt, Maryland.
Reber, C. A. and Hays, P. B.: 1973, *J. Geophys. Res.* **78**, to be published.
Reber, C. A. and Nicolet, M.: 1965, *Planetary Space Sci.* **13**, 617.
Reber, C. A., Cooley, J. E., and Harpold, D. N.: 1968, *Space Res.* **8**, 993.
Reber, C. A., Harpold, D. N., Horowitz, R., and Hedin, A. E.: 1971, *J. Geophys. Res.* **76**, 1845.
Samson, J. A. R.: 1966, in D. R. Bates and I. Estermann (eds.), *Advances in Atomic and Molecular Physics*, vol. 2, Academic Press, New York, pp. 177–261.
Samson, J. A. R.: 1969, *Phys. Rev. Letters* **22**, 693.
Schmucker, U.: 1969, in K. H. Wedepohl (ed.), *Handbook of Geochemistry*, vol. I, Springer-Verlag, Berlin, pp. 134–226.
Schram, B. L., De Heer, F. J., Van der Wiel, M. J., and Kistemaker, J.: 1965, *Physica* **31**, 94.
Schram, B. L., Moustafa, H. R., Schutten, J., and De Heer, F. J.: 1966, *Physica* **32**, 734.
Secchi, P.: 1868, *Compt. Rend. Acad. Sci. Paris* **67**, 1123.
Shefov, N. N.: 1961, *Ann. Geophys.* **17**, 395.
Sheldon, W. R. and Kern, J. W.: 1972, *J. Geophys. Res.* **77**, 6194.
Signer, P. and Suess, H. E.: 1963, in E. D. Goldberg and J. Geiss (eds.), *Earth Science and Meteoritics*, North-Holland Publishing Company, Amsterdam, pp. 241–272.
Taylor, H. A., Jr.: 1971, *Planetary Space Sci.* **19**, 77.
Taylor, H. A., Jr.: 1972, *Planetary Space Sci.* **20**, 1593.
Taylor, H. A., Jr., Brace, L. H., Brinton, H. C., and Smith, C. R.: 1963, *J. Geophys. Res.* **68**, 5339.
Timothy, A. F. and Timothy, J. G.: 1970, *J. Geophys. Res.* **75**, 6950.
Turekian, K. K.: 1959, *Geochim. Cosmochim. Acta* **17**, 37.
Victoreen, J. A.: 1949, *J. Appl. Phys.* **20**, 1141.
Warneck, P.: 1967, J. *Chem. Phys.* **47**, 4279.
Wasserburg, G. J., MacDonald, G. J. F., Hoyle, F., and Fowler, W. A.: 1964, *Science* **143**, 465.
Wasserburg, G. J., Mazor, E., and Zartman, R. E.: 1963, in E. D. Goldberg and J. Geiss (eds.), *Earth Science and Meteoritics*, North-Holland Publishing Company, Amsterdam, pp. 219–240.
Watson, H. E.: 1910, *J. Chem. Soc. London* **97**, 810.
Wood, A. T., Jr., Noyes, R. W., Dupree, A. K., Huber, M. C. E., Parkinson, W. H., Reeves, E. M., and Withbroe, G. L.: 1972, *Solar Phys.* **24**, 169.
von Zahn, U.: 1970, *J. Geophys. Res.* **75**, 5517.
Zimmerman, S. P., Faire, A. C., and Murphy, E. A.: 1972, *Space Res.* **12**, 615.